The Institute of Paper Chemistry

Appleton, Wisconsin

Doctor's Dissertation

The Configuration and Hydrodynamic Properties of Fully Acetylated Salep Glucomannan

David H. Juers

June, 1965

THE CONFIGURATION AND HYDRODYNAMIC PROPERTIES OF FULLY ACETYLATED SALEP GLUCOMANNAN

A thesis submitted by

David H. Juers

B.S. 1960, The Pennsylvania State University
M.S. 1962, Lawrence College

in partial fulfillment of the requirements
of The Institute of Paper Chemistry
for the degree of Doctor of Philosophy
from Lawrence University,
Appleton, Wisconsin

June, 1965

TABLE OF CONTENTS

SUMMARY

Studies of the solution properties of polymers reveal that cellulose and its derivatives are more extended than vinyl polymers of equal contour length. However, very little study has been made of the β-1,4-linked polysaccharides with sugars other than D-glucose in the backbone of the molecule. It has been shown that fully acetylated guaran has the same configuration as the cellulosics. However, its hydrodynamic properties are such that it changes from partial free-draining to nondraining with increasing degrees of polymerization, and this hydrodynamic transition has not been observed for the cellulosics. The purpose of the thesis is to study the configuration and hydrodynamic properties of a β-1,4-linked polysaccharide with both D-glucose and D-mannose in the polymer chain, and to compare the effect of the α-1, 6-galactose side group on the hydrodynamic properties of guaran triacetate.

The β-1,4-linked natively acetylated (2%) polysaccharide previously called salep mannan was shown in this study to be a glucomannan by the chromatographic identification, with authentic knowns, of 4-O-β-D-glucosidomannose and 4-O-β-D-mannosidoglucose from the partial acid hydrolyzate of the polymer, and by the establishment of the constancy of the mannose-to-glucose ratio at 2.7 when the glucomannan was fractionally precipitated by barium complex formation.

The fully acetylated glucomannan was fractionally precipitated into 21 fractions with the following characteristics in nitroethane: number-average degrees of polymerization, by osmometry, from 268 to 3210; weight-average degrees of polymerization, by light scattering, from 615 to 4170; and intrinsic viscosities from 122 to 625 ml./g. The viscosities of the high molecular weight fractions were corrected for non-Newtonian flow behavior.

The dependence of the radius of gyration on the contour length of salep glucomannan triacetate is the same as that for cellulose tricaproate, hydroxyethyl

cellulose, and guaran triacetate, indicating that the β-1, 4-linked chains of D-glucose, D-mannose, or mixtures of D-glucose and D-mannose have similar configurations in spite of the structural differences of the anhydrosugar units. The similarity of the configurations of salep glucomannan triacetate and guaran triacetate is also demonstrated by the nearly equal persistence lengths of the Porod-Kratky chain model (55.1 A. and 57.8 A., respectively) obtained from the analyses of the intrinsic viscosity – degree of polymerization data according to the Eizner-Ptitsyn theory.

As interpreted by the Eizner-Ptitsyn theory, the intrinsic viscosity – degree of polymerization relationship for salep glucomannan triacetate is affected by two factors, the partial permeability of the solvent into the molecule, and the change of the geometric factor with degree of polymerization. Scatter in the data makes it impossible to assign an accurate value to the hydrodynamic monomer radius, $\underline{r}_o$, but it is in the range of 0.55 to 2.73 A. A value of 3.05 A. was found for guaran triacetate. The nondraining behavior of guaran triacetate is caused by its larger monomeric friction coefficient and the fact that the geometric factor has reached its high molecular weight limit of 1.0.

Calculation of the radius of gyration from the Eizner-Ptitsyn theory indicates that it is necessary to distinguish between the hydrodynamic and light-scattering radius of gyration. The Flory coefficient, Φ, calculated from the Eizner-Ptitsyn theory, is lower than its limiting value and increases with increasing molecular weight. This behavior reflects the non-Gaussian configuration and the hydrodynamic permeability of salep glucomannan triacetate, and indicates that the molecule tends toward the limiting conditions of spherical symmetry and total internal resistance to flow. When the hydrodynamic radius of gyration is used to calculate Φ from experimental data, agreement with the theoretical Eizner-Ptitsyn values is obtained.

Calculation of Φ from the light-scattering radius of gyration yields values which are lower than the theoretical values. Polymolecularity was estimated from osmometry and light-scattering data using the Zimm-Schulz type distribution.

INTRODUCTION

Studies of the solution properties of cellulose and its derivatives have revealed that these β-1, 4-linked polysaccharides are much more extended than vinyl polymers of comparable contour length. The extended nature of the cellulosics is reflected in the high viscosity of their dilute solutions and in their large size as determined by light-scattering measurements. This characteristic extension complicates the interpretation of the polymer's molecular properties in dilute solutions, and none of the hydrodynamic theories which hold for vinyl polymers (1-6) adequately describe the cellulosics. The recent theory of Eizner and Ptitsyn (7) assumes an extended molecular model, which the others do not do, and this results in a more satisfactory interpretation of the hydrodynamic properties of semirigid molecules, like cellulose.

The β-1, 4-linked polysaccharides other than the cellulosics have received very little hydrodynamic study. Little was known about how sugars other than glucose in the backbone of the molecule affect the molecular configuration and hydrodynamic properties of β-1, 4-linked polysaccharides until Koleske (8) studied the acetate derivative of guaran, a linear mannan with α-1, 6-galactose groups on every other mannose unit. Later, Kurath, Schmitt, and Bachhuber (9) analyzed Koleske's data according to the Eizner-Ptitsyn theory. The results of these investigations show that the guaran triacetate has a chain conformation very similar to cellulosics, but its hydrodynamic properties are quite different, being partially free-draining at low DP and nondraining at high DP. This transition from partial free-draining to nondraining has not been observed for the cellulosics.

The present study was undertaken to broaden the understanding of the hydrodynamic properties of β-1, 4-polysaccharides, and in particular to investigate

the effect of the galactose side group on the hydrodynamic properties of the β-1,4-linked mannan. Previous work (10) indicated that the polymer chosen for the present study, known as salep mannan, is a water-soluble natively acetylated β-1, 4-mannan obtained from the tubers of certain species of Orchis. However, early in the experimental work it was shown that the polymer is a glucomannan, which is in agreement with the findings of other workers (11-13). As a result, this is the first hydrodynamic study of a high molecular weight β-1,4-linked heteroglycan.

THEORETICAL

INTRODUCTION

The most obvious characteristic of a polymer solution is that its viscosity is much larger than that of the pure solvent. In 1930 Staudinger (14) suggested that the relative magnitude of this viscosity increase could be quantitatively related to the molecular weight of the polymeric solute. Since then, both theory and experiment have proved the essential validity of Staudinger's suggestion. The exact theory of polymer solution is still in the formative stage, and the viscosity determination of molecular weights must be calibrated by an absolute method. However, for known viscosity – molecular weight relationships, the viscosity method is the easiest and most rapid for determining molecular weights.

GENERAL

The viscosity of a fluid is that property which determines the resistance to motion when a shearing force is exerted on the fluid under laminar flow conditions. The high viscosity of polymer solutions is a result of the hydrodynamic resistance caused by polymer molecules as they perturb the flow of the surrounding medium. The perturbation caused by the polymer molecule depends on the viscosity of the solvent, the degree of polymerization, the monomeric friction coefficient, and the size of the molecule, which may be represented by the root-mean-square distance, $(\overline{S^2})^{1/2}$ of a monomer unit from the center of gravity. The general theoretical approach is to relate these various factors to the intrinsic viscosity of a polymer solution.

Theories for treating the intrinsic viscosity of polymer solutions have been developed by Debye and Bueche (1), Kirkwood and Riseman (2), Kurata and Yamakawa (3), Peterlin (4), Kuhn and Kuhn (5), Flory and Fox (6), and Eizner and Ptitsyn

(7). All but the Eizner and Ptitsyn theory fail to adequately describe the experimental data of β-1,4-linked polysaccharides because the molecular models of these theories do not account for the stiffness of the polysaccharide chain. However, the Eizner-Ptitsyn theory, which uses the Porod-Kratky "wormlike" chain model (15) to describe the conformation properties of semirigid molecules, has been shown to adequately describe the experimental data of β-1,4-linked polysaccharides (7, 9).

EIZNER-PTITSYN THEORY

Eizner and Ptitsyn (7) have treated the intrinsic viscosity of semirigid macromolecules in light of the intrinsic viscosity equation of Peterlin (4, 16),

$$[\eta] = N_A \overline{(S^2)}\, N\zeta \Big/ \left(\pi 6M\, \eta_o [1 + \{4\zeta/(9\pi\eta_o N^2)\} \sum_{t=1}^{N/2} \sum_{p=1}^{N} (N-2p)(\overline{1/r_{pt}})]\right) \quad (1),$$

where N_A is Avogadro's number, $\overline{(S^2)}$ is the mean-square radius of gyration of the molecule, M is its molecular weight, and N is its degree of polymerization, ζ is the monomeric friction coefficient, η_o is the viscosity of the solvent, and r_{pt} is the distance between monomeric units p and t. By using the "wormlike" chain of Porod and Kratky (15) to evaluate $(\overline{1/r_{pt}})$, Eizner and Ptitsyn derive the following equation for intrinsic viscosity:

$$[\eta] = \frac{2^{3/2}\, \Phi_o\, (b^3/M_o)\, N\, X\, (N/\lambda)}{1.285\, [b/r_o\lambda] + [1/\lambda^{3/2}]\, \Phi\, (\lambda, N)\, N^{1/2}} \quad (2),$$

where $[\eta]$ is the intrinsic viscosity in ml./g., Φ_o is the Flory coefficient whose limiting value is 2.86×10^{23} mole^{-1} at high molecular weight (7), r_o is the hydrodynamic radius of the monomer unit and M_o is its molecular weight, b

is the length of the monomer unit, and $\lambda = \underline{a}/\underline{b}$. The persistence length of the Porod-Kratky wormlike chain, $\underline{a}$, is a measure of the "stiffness" of the molecule. It is defined by $\underline{a} = -\underline{b}/\ln \overline{\cos \alpha}$, where α is the supplement of the angle between successive monomer units. The geometric factor $\underline{X}(\underline{N}/\lambda)$ and the hydrodynamic function $\Phi\ (\lambda, \underline{N})$, complex functions of λ and $\underline{N}$, have been calculated and presented in graphical form by Eizner and Ptitsyn (7). Since they do not present the numerical results, their graphs cannot be reproduced easily. The geometric factor can be calculated by hand, from the following equation:

$$X(N/\lambda) = 1 - [3/(N/\lambda)^3] \left\{(N/\lambda)^2 - 2[(N/\lambda) - 1 + e^{-(N/\lambda)}]\right\} \qquad (3).$$

The hydrodynamic function, $\Phi\ (\lambda, \underline{N})$, much too complex for hand calculation, has been calculated by numerical summation on an IBM 1620 computer, and the numerical results have been presented by Kurath, et al. (9). Above $\underline{N} \cong 50$ $\Phi\ (\lambda, \underline{N})$ decreases with increasing $\underline{N}$ and increases with increasing chain rigidity. For flexible polymers, $(\lambda \cong 4)$, the effect of both factors on $\Phi\ (\lambda, \underline{N})$ is compensated and the intrinsic viscosity conforms to the theories of Peterlin (4) and Kirkwood and Riseman (2). As $\underline{N}$ approaches infinity $\Phi\ (\lambda, \underline{N})$ approaches 1 and the intrinsic viscosity again conforms to the Peterlin and Kirkwood-Riseman theories.

The Flory coefficient is defined by (6, 17),

$$\Phi = [\eta]\, \overline{M}_n / 6(\overline{s_n^2})^{3/2} \qquad (4).$$

According to the Eizner-Ptitsyn theory, the Flory coefficient is given by,

$$\Phi = \Phi_o \Big/ \left\{\Phi(\lambda, N) + [45(2\pi/3)^{1/2}]/[32(3-2^{1/2})]\ b/r_o\ (\lambda/N)^{1/2}\right\} X^{1/2}(N/\lambda) \qquad (5).$$

It can be seen that molecular extension, measured by λ, as well as solvent permeability, measured by $\Phi\ (\lambda, \underline{N})$, decreases the value of Φ as compared to that for the Gaussian coil.

The techniques of applying experimental data to the Eizner-Ptitsyn theory will be presented in the discussion section.

EXPERIMENTAL PROCEDURES AND RESULTS

ISOLATION OF THE GLUCOMANNAN FROM TUBERA SALEP

The natively acetylated glucomannan was isolated from powdered Tubera salep (The Meer Corporation, New York, New York) according to a modified procedure of Husemann (10). Approximately 10 g. of the powdered tuber (4.97% moisture) was refluxed in 500 ml. of methanol for 1 hr. to inactivate enzymes, was filtered and washed with methanol, ethyl ether, and petroleum ether, and dried under vacuum at 25°C. for 2 hr. The filtrate was added to 1.5 liters of distilled water and extracted, in the dark, by stirring. The resultant solution was clarified using a Sharples Super Centrifuge at 42,000 r.p.m. The yield of water-extractable polymer varied from 54 to 62%, based on the oven-dried enzyme-inactivated powder.

The occurrence of a slight blue color upon the addition of 0.01N iodine solution to the clarified polymer solution suggested the presence of a small amount of starch. Ten milligrams of alpha amylase (Nutritional Biochemicals Corporation, Cleveland, Ohio) was added to 1.5 liters of the clarified solution and was permitted to react for 3 hr. This procedure resulted in a negative starch test, and did not seem to significantly degrade the polymer. The intrinsic viscosities of the enzyme-hydrolyzed and the unhydrolyzed solutions were 1530 and 1580 ml./g., respectively.

After alpha amylase treatment, the polymer was precipitated as a fibrous white material by adding the solution slowly, with stirring, to three volumes of methanol. Later (24 hr.) the precipitate was filtered, redissolved in water, and freeze dried. Yields of the white fluffy polymer varied from 29 to 39% for six batches, and a total of 20.3 g. of ash-free polymer was isolated.

CHEMICAL CHARACTERIZATION OF THE POLYMER

COMPLETE ACID HYDROLYSIS

The polymer was subjected to acid hydrolysis and qualitative chromatography according to a modified procedure of Saeman, et al. (18). See Appendix I for a description of the developers and sprays used. Heavy spotting of the hydrolyzate indicated the presence of large quantities of mannose and glucose, trace amounts of faster moving compounds (termed "A", "B", and "C"), and the absence of acidic materials. The mobilities of the spots relative to the solvent front, R_f, are given in Table I. It will be shown later that mannose and glucose comprise 96% of the glucomannan.

TABLE I

R_f VALUES OF COMPOUNDS IN SALEP GLUCOMANNAN ACID HYDROLYZATE

Compound	R_f
Glucose	0.139
Mannose	0.181
Unknowns	
A	0.527
B	0.576
C	0.855

The hydrolyzate was separated paper chromatographically and the areas corresponding to glucose and mannose knowns were eluted with distilled water. The optical rotations of the elutants were positive, showing that the eluted sugars were dextrorotatory. The phenylhydrazone derivative prepared from the eluted mannose had a decomposition range from 185 to 187°C., in agreement with the decomposition range of 184 to 186°C. for authentic D-mannose phenylhydrazone.

GRADED ACID HYDROLYSIS

The glucomannan was subjected to graded acid hydrolysis in 1N sulfuric acid at 70°C. for 8 hr. according to the method of McKee (19). A qualitative paper chromatographic investigation of the hydrolyzate was performed by running several authentic known compounds concurrently. It has been shown that these known compounds exist in the graded acid hydrolyzates of wood glucomannans (20-23), and thus could be expected in the graded acid hydrolyzate of salep glucomannan. The mobilities of the known and unknown compounds relative to glucose, R_{gl}, are given in Table II.

TABLE II

R_{gl} VALUES OF THE KNOWN AUTHENTIC REFERENCE COMPOUNDS AND THE UNKNOWN COMPOUNDS IN THE GRADED ACID HYDROLYZATE OF SALEP GLUCOMANNAN

Known Compounds	R_{gl}
D-mannose	1.27
D-glucose	1.00
Glucosidomannose (4-O-β-D-glucopyranosyl-β-D-mannopyranose)	0.615
Cellobiose	0.370
Mannobiose	0.358
Mannosidoglucose (4-O-β-D-mannopyranosyl-β-D-glucopyranose)	0.220
Mannotriose	0.078
Unknown Compounds in Graded Hydrolyzate	
D(medium)	1.27
E(medium-faint)	1.00
F(medium)	0.612
G(medium)	0.364
H(faint)	0.225
J(faint)	0.078

The hydrolyzate was separated paper chromatographically and the area corresponding to the R_{gl} of 0.612 was eluted with water. Hydrolysis of the extracted disaccharide with 3% sulfuric acid in an autoclave at 15 p.s.i.g. for 1 hr. and

chromatographic separation indicated only the presence of approximately equal amounts of glucose and mannose. Similar elution, hydrolysis, and chromatography of the material corresponding to the R_{gl} range of 0.358-0.370 indicated the presence of an appreciable quantity of mannose and a trace amount of glucose, thereby suggesting the presence of mannobiose and a trace of cellobiose in the graded acid hydrolyzate.

The information in Table II together with that obtained from the disaccharide elutions, hydrolysis, and chromatography suggests that the hydrolyzate contains all of the possible mono- and disaccharides, and one of the possible trisaccharides that would be expected from a graded hydrolysis of a β-1,4-linked glucomannan.

BARIUM PRECIPITATION OF THE GLUCOMANNAN

To investigate the possibility that the polymer isolated by water extraction of powdered Tubera salep is a mannan – glucomannan mixture, it was fractionated by barium complex formation which has been shown to precipitate mannans and glucomannans (24). A dilute polymer solution was made 0.2N in sodium hydroxide and following Vaughan's procedure (25) was precipitated with 2.14M barium acetate. As suggested by Thompson (26), the barium acetate was added slowly until the solution became turbid. The precipitated complex was filtered and additional barium acetate was added to the supernatant solution. This procedure was repeated until the addition of barium acetate caused no turbidity, yielding a total of three fractions. Each precipitated complex was dissolved in 1N acetic acid and the polymer was precipitated by the addition of 95% ethanol. After 24 hr. the polymer was filtered and solvent exchanged with absolute ethanol, ethyl ether, and petroleum ether; air dried; and vacuum dried at 30°C.

The relative amounts of mannose and glucose in the whole polymer and the barium-precipitated fractions were determined by the technique of Saeman, et al. (18). The results are given in Table III.

TABLE III

MANNOSE-TO-GLUCOSE RATIOS IN THE UNFRACTIONATED POLYMER AND THE BARIUM-PRECIPITATED FRACTIONS

Sample	Mannose-to-Glucose Ratio
Unfractionated polymer	2.63
Barium fraction No. 1	2.78
Barium fraction No. 2	2.70
Barium fraction No. 3	2.85
Average	2.74 $\pm$ 0.11

The differences in the sugar ratios given in Table III are within experimental error. If the polymer were a mannan – glucomannan mixture it would be expected that the sugar ratios of the barium-precipitated fractions would be significantly different from each other and the unfractionated polymer. Since the ratios are not different the polymer is presumably homogeneous.

ANALYSIS OF THE GLUCOMANNAN

In addition to the mannose-to-glucose ratios given in Table III, the results of quantitative analyses of the glucomannan for sugars (18), nitrogen (27), and acetyl (28) are given in Table IV.

OPTICAL ROTATION

The optical rotation of the glucomannan in 6% sodium hydroxide at 25°C. was determined with a Zeiss-Winkle polarimeter giving

$$[\alpha]_D^{25} = -43.3°.$$

This is in good agreement with the value of -44° found by Husemann (10).

TABLE IV

RESULTS OF QUANTITATIVE ANALYSIS OF SALEP GLUCOMANNAN

Glucose	26.6 ± 1.0%
Mannose	69.5 ± 2.0%
Galactose	< 0.5
Unknown compounds	
A	< 0.5
B	< 0.5
C	< 0.5
Acetyl	2.1 ± 0.2%
Nitrogen	0.11 ± 0.01%

PREPARATION OF SALEP GLUCOMANNAN TRIACETATE

The acetate derivative of the glucomannan was prepared by the method of Carson and Maclay (29), which has been shown to yield a fully acetylated polysaccharide derivative (8, 29). Based on the triacetate, the yield of the derivative was 88.5% of theoretical. The white fluffy product had a melting point range from 242 to 248°C.

The acetyl content of the glucomannan acetate as determined by (a) the Eberstadt method, a long saponification at approximately 25°C. (30), and (b) transesterification using sodium methoxide in methanol (28) was 45.2 ± 0.2% and 42.6 ± 0.2%, respectively. Theoretical acetyl content of the glucomannan triacetate is 44.8%. The former of the two experimental values was considered the more reliable.

SOLVENT PURIFICATION

Nitroethane, the solvent selected (see Appendix II) for viscosity and molecular weight measurements of salep glucomannan triacetate, can be purified to 99.5% purity by careful distillation (31). It was double distilled using a 30-inch glass column (I.D.=0.75 in.) packed with 1/4 by 1/32 in. glass helices. Three liters of practical grade nitroethane (Matheson, Coleman, and Bell Company) were refluxed over Drierite at a 0.9 reflux ratio until a constant temperature of 112°C. was attained in the distilling head, and the 200 ml. of the initial distillate, boiling below 112°C., was discarded. The solvent was then distilled at a reflux ratio of 0.67 until 1.5 liters were obtained. The singly distilled nitroethane was redistilled in the same manner, yielding 1 liter of pure solvent at a boiling point of 112°C. It was stored in a glass-stoppered bottle in the dark at 22°C.

FRACTIONATION OF SALEP GLUCOMANNAN TRIACETATE

Fractional precipitation (32-36) was employed to fractionate the salep glucomannan triacetate. The polymer (9.83 g.) was dissolved in practical-grade nitroethane to yield a 0.19% solution. Fractions were obtained by adding high boiling petroleum ether (b.p. = 65-110°C.) slowly to the agitated solution until turbidity was observed. After heating to 35°C. to effect solution the system was permitted to cool slowly to 22°C. where it was maintained (8 to 24 hr.) until the precipitated polymer had settled. The supernatant solution was siphoned off. The polymer, collected by centrifugation, was added to petroleum ether, under agitation, in a tared beaker. The ether was evaporated and the polymer dried under vacuum at 40°C. for 120 hr. With the exceptions of Fractions 4G and 14, which were obtained by evaporation of the final precipitation solution, this procedure was repeated for all the fractions listed in Table V.

TABLE V

RESULTS OF THE FRACTIONATION OF SALEP GLUCOMANNAN TRIACETATE FROM A NITROETHANE SOLUTION WITH PETROLEUM ETHER

Fraction Number	Fraction Weight, g.	Fraction Number	Fraction Weight, g.
1	0.107	5	1.354
2	0.045	6	0.100
3	0.122	7	0.120
4[a]	3.274	8	0.929
4A	0.134	9	0.598
4B	1.208	10	0.620
4C	0.206	11	0.860
4D	0.510	12	0.878
4E	0.180	13	0.340
4F	0.675	14	0.978
4G	0.485		

% Recovery = 10.45/9.83 = 106

[a]Fraction 4 was refractionated into seven fractions designated as Fractions 4A through 4G.

Fraction 4 contained 33.3% of the starting polymer and was refractionated from a 0.22% solution to yield seven fractions. Fraction 4A was almost entirely dust and dirt that had been suspended in the precipitation solution, and it was discarded.

VISCOMETRY

Viscosity measurements were conducted at 30.00 ± 0.01°C. in a modified Ubbelohde four-bulb variable shear viscometer (8, 37, 38). Drainage and end effect errors (39) were neglected and kinetic energy corrections (see Appendix III), calculated to be less than 0.5%, were considered negligible.

The intrinsic viscosities were determined according to the equations (40),

$$\eta_{sp}/c = [\eta] + k_1 [\eta]^2 c \qquad (6),$$

and

$$(\ln \eta_{rel})/c = [\eta] - k_2 [\eta]^2 c \qquad (7),$$

by plotting η_{sp}/c and $(\ln \eta_{rel})/c$ versus concentration as shown in Fig. 1-5.

The shear stress τ_R in dynes/sq. cm. at the wall of the capillary of radius R and length L is given by (41),

$$\tau_R = h\rho gR/2L \qquad (8),$$

where ρ is the solution density and h is the mean hydrostatic head calculated from Meissner's equation (38),

$$h = (m_1 - m_2)/\ln(m_1/m_2) \qquad (9).$$

Here, m_1 and m_2 refer to the height of the hydrostatic head from the top and bottom of a bulb, respectively. Therefore, for a given viscometer and a particular bulb,

$$\tau_R = (\text{constant})\ \rho \qquad (10).$$

For those solutions displaying non-Newtonian behavior the apparent relative viscosities η_{rel}* were plotted as a function of shear stress and extrapolated to zero shear stress for each concentration, as shown in Fig. 6. The zero shear stress intercepts were then used to determine the intrinsic viscosities according to Equations (6) and (7). Unfractionated salep glucomannan triacetate and

*Fractions 1 and 2 combined for the viscosity measurement.

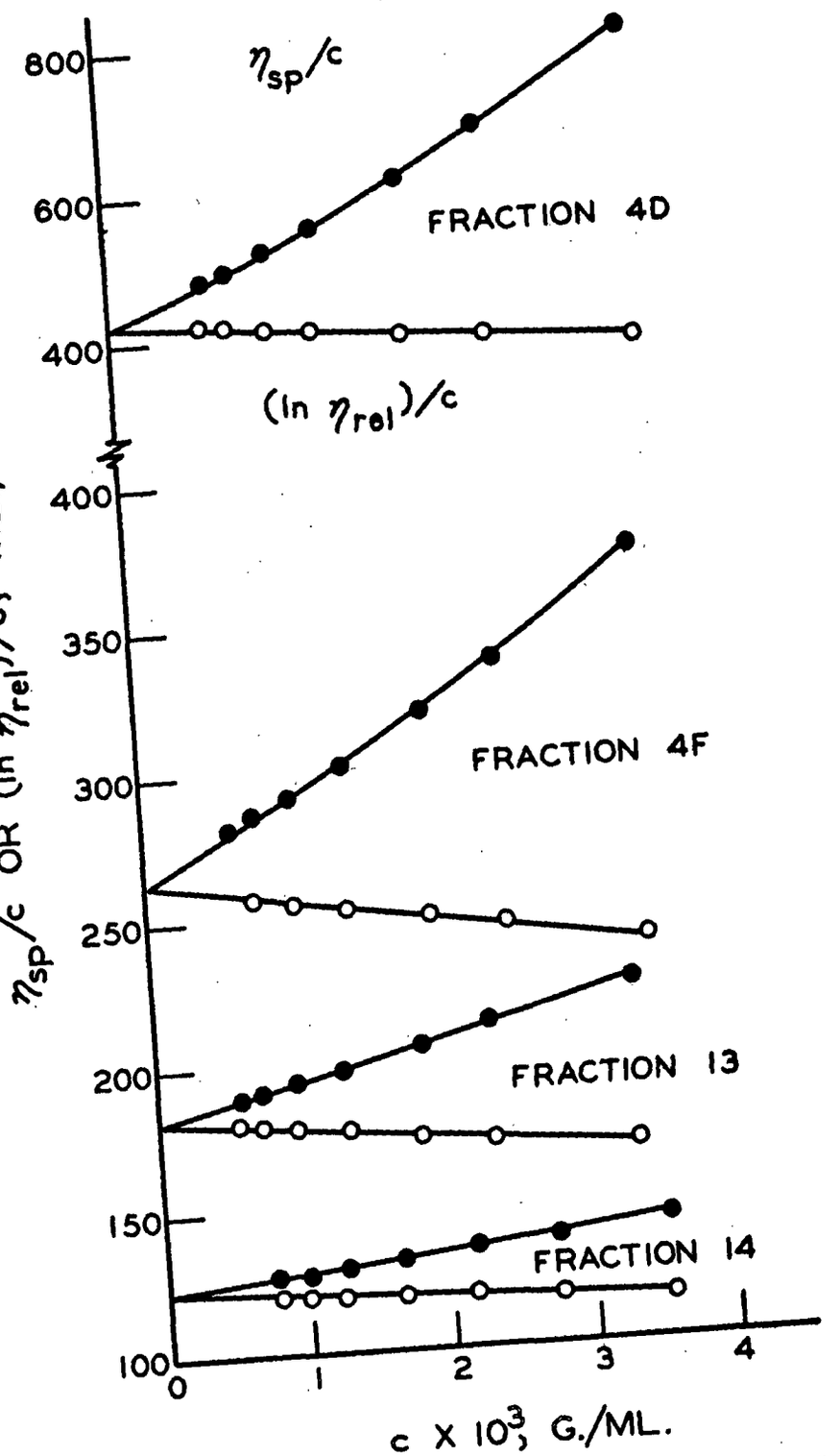

Figure 1. Double Plot of $\eta_{sp}/\underline{c}$ (Solid Circles) and $(\ln \eta_{rel})/\underline{c}$ (Open Circles) as a Function of Concentration for Salep Glucomannan Triacetate in Nitroethane at 30°C. for Fractions 4D, 4F, 13, and 14

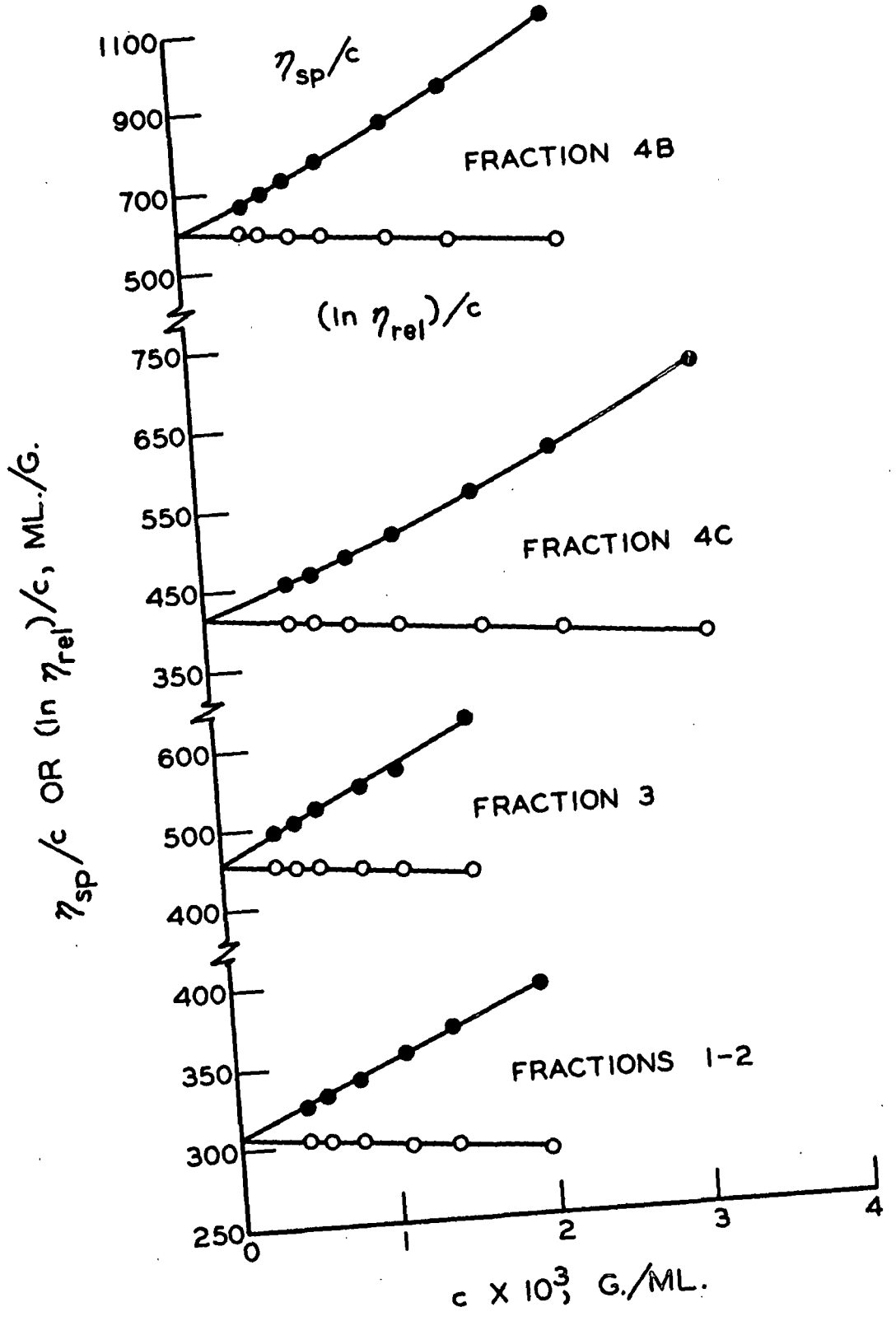

Figure 2. Double Plot of $\eta_{sp}/\underline{c}$ (Solid Circles) and $(\ln \eta_{rel})/\underline{c}$ (Open Circles) as a Function of Concentration for Salep Glucomannan Triacetate in Nitroethane at 30°C. for Fractions 1-2, 3, 4B, and 4C

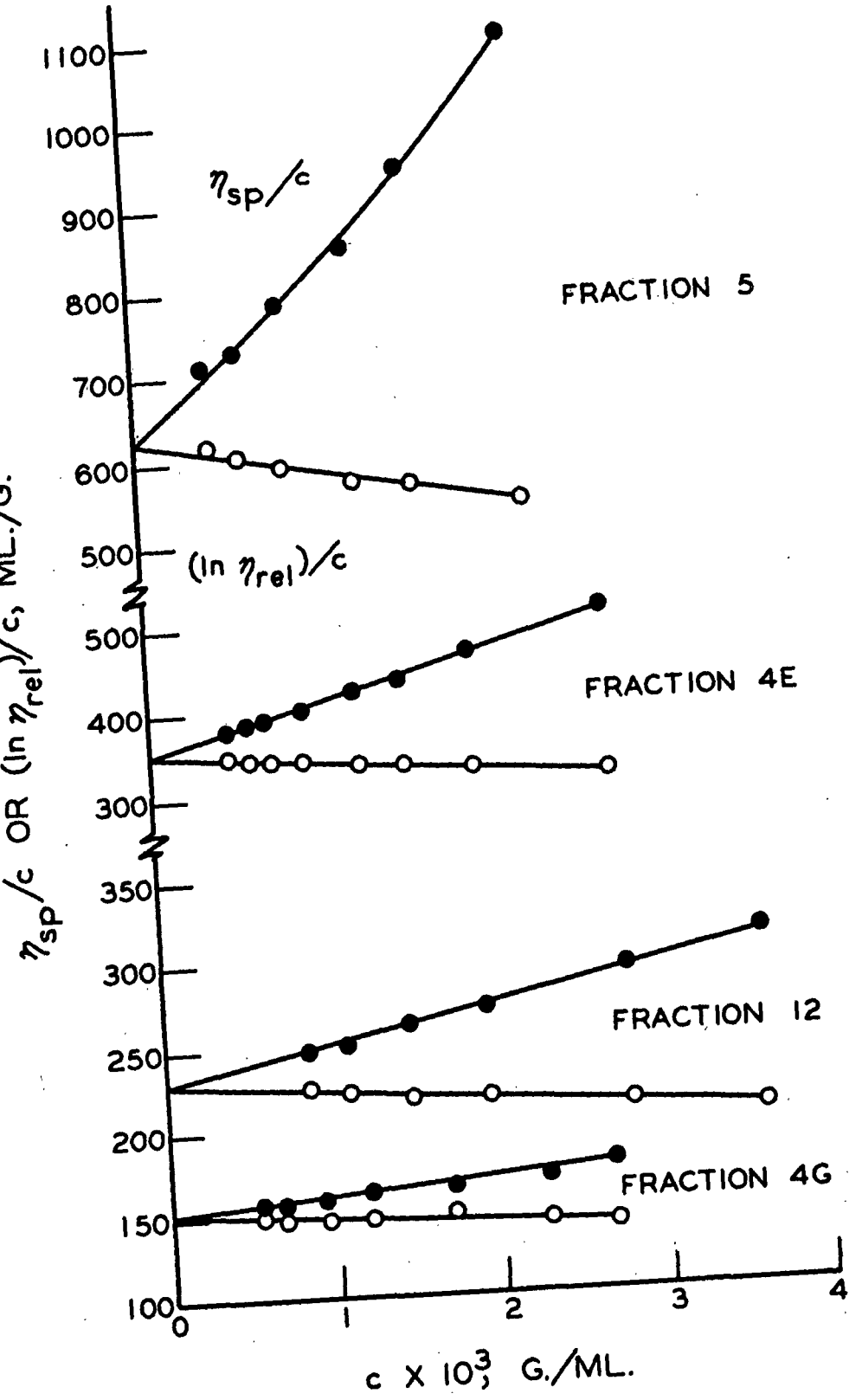

Figure 3. Double Plot of $\eta_{sp}/\underline{c}$ (Solid Circles) and $(\ln \eta_{rel})/\underline{c}$ (Open Circles) as a Function of Concentration for Salep Glucomannan Triacetate in Nitroethane at 30°C. for Fractions 4E, 4G, 5, and 12

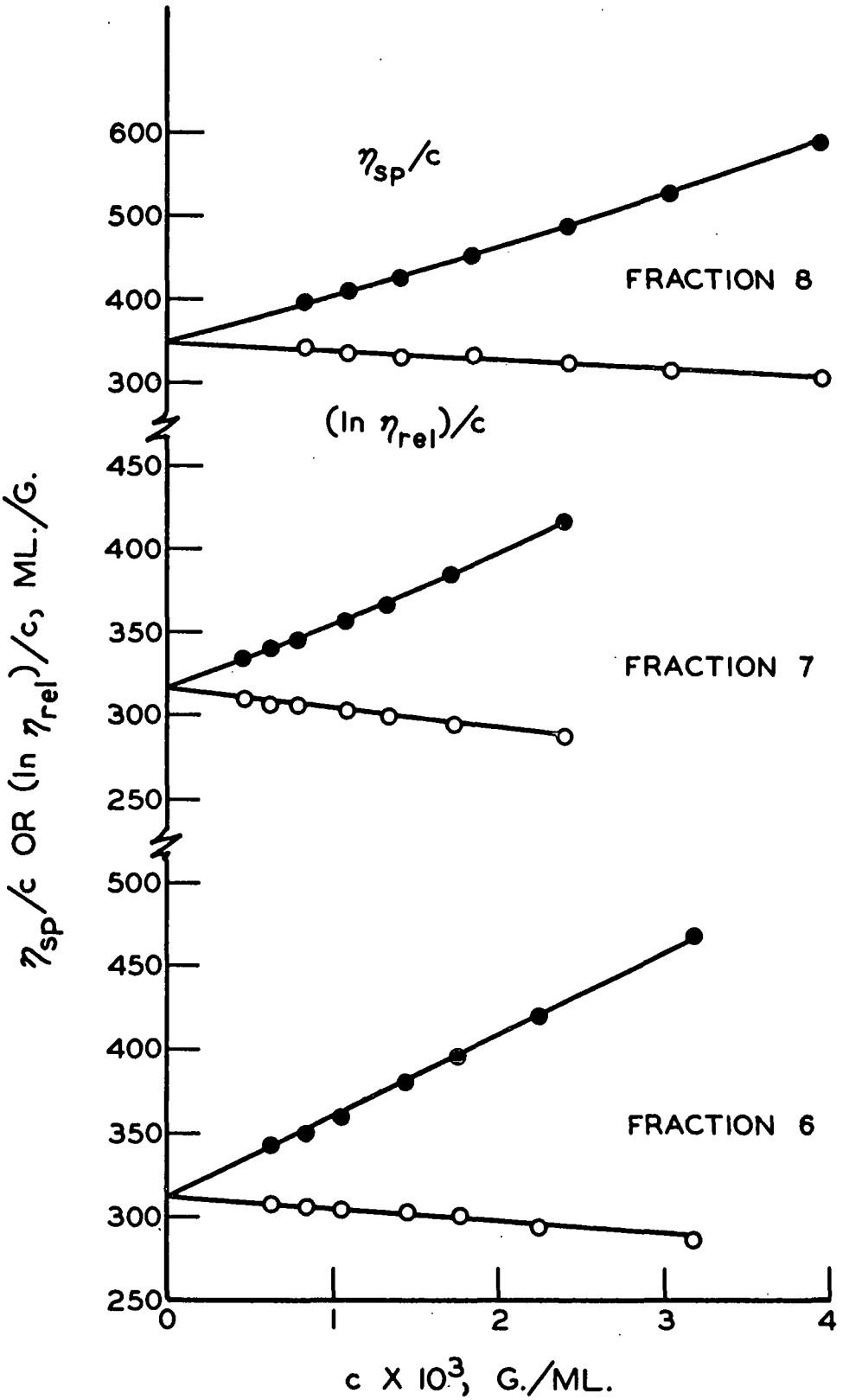

Figure 4. Double Plot of $\eta_{sp}/\underline{c}$ (Solid Circles) and $(\ln \eta_{rel})/\underline{c}$ (Open Circles) as a Function of Concentration for Salep Glucomannan Triacetate in Nitroethane at 30°C. for Fractions 6, 7, and 8

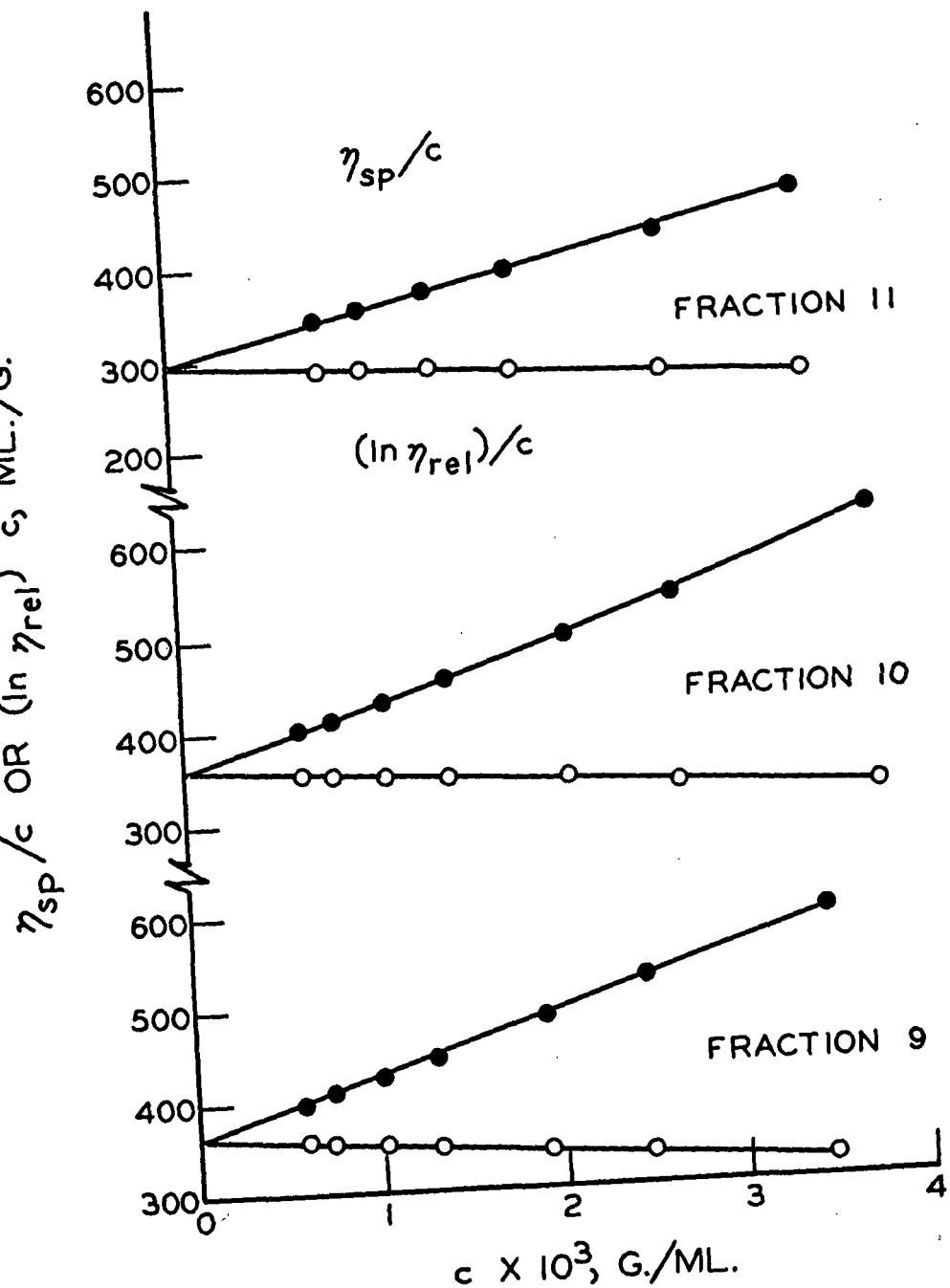

Figure 5. Double Plot of $\eta_{sp}/\underline{c}$ (Solid Circles) and $(\ln \eta_{rel})/\underline{c}$ (Open Circles) as a Function of Concentration for Salep Glucomannan Triacetate in Nitroethane at 30°C. for Fractions 9, 10, and 11

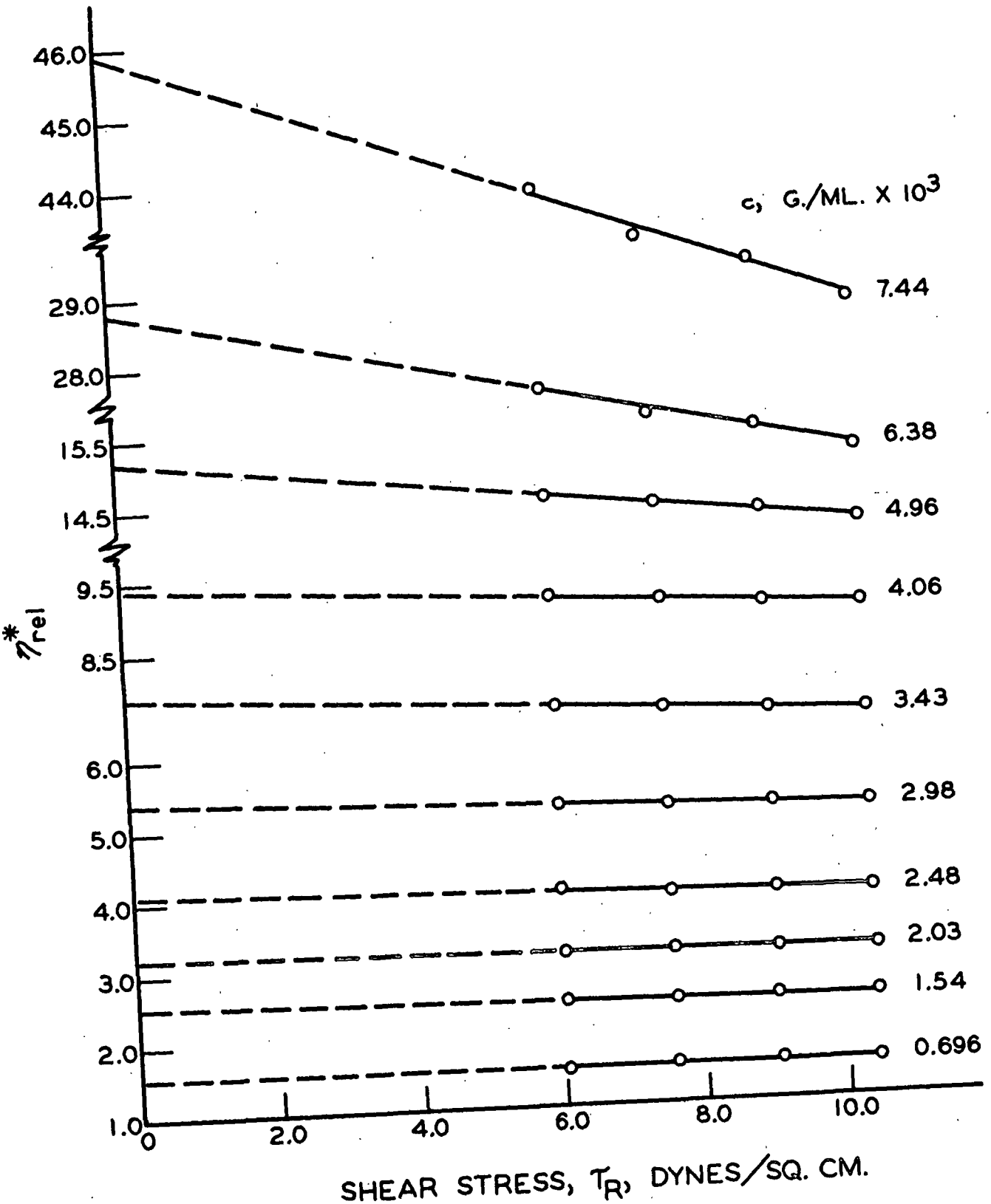

Figure 6. Apparent Relative Viscosity as a Function of Shear Stress for Unfractionated Salep Glucomannan Triacetate in Nitroethane at 30°C.

Fractions 5 and 4B, with intrinsic viscosities above 605 ml./g., were the only ones to display non-Newtonian behavior. The intrinsic viscosities are given in Table VI.

TABLE VI

INTRINSIC VISCOSITIES OF SALEP GLUCOMANNAN TRIACETATE IN NITROETHANE AT 30°C.

Fraction Number	Intrinsic Viscosity, ml./g.	Fraction Number	Intrinsic Viscosity, ml./g.
Unfractionated	630	6	312
1-2[a]	308	7	313
3	461	8	348
4B	605	9	365
4C	416	10	362
4D	428	11	295
4E	350	12	228
4F	263	13	182
4G	152	14	122
5	625		

[a]Fractions 1 and 2 combined for the viscosity measurement.

In fractional precipitation the high molecular weight materials should be precipitated first, and one would expect the intrinsic viscosity to decrease with increasing fraction number. On this basis, Fractions 1-2, 3, 4C, 6, and 7 all have intrinsic viscosities which appear to be too low. There is reason to believe that these six fractions underwent some degradation. They were stored for six months before the viscosity measurements were made, and it appeared as if moisture had collected in the bottles, though they were tightly capped. Reaction of the water with any residual acetic anhydride from the acetylation procedure could

have formed acetic acid which could degrade the polymer. For the other fractions, the storage time before measurements were made was much less, and degradation was not apparent.

OSMOMETRY

Osmotic pressure measurements were made in nitroethane using a Mechrolab High Speed Membrane Osmometer, Model 501 (42), schematically represented in Fig. 7. The instrument is thermostated so that the standard operating temperature is 37°C.

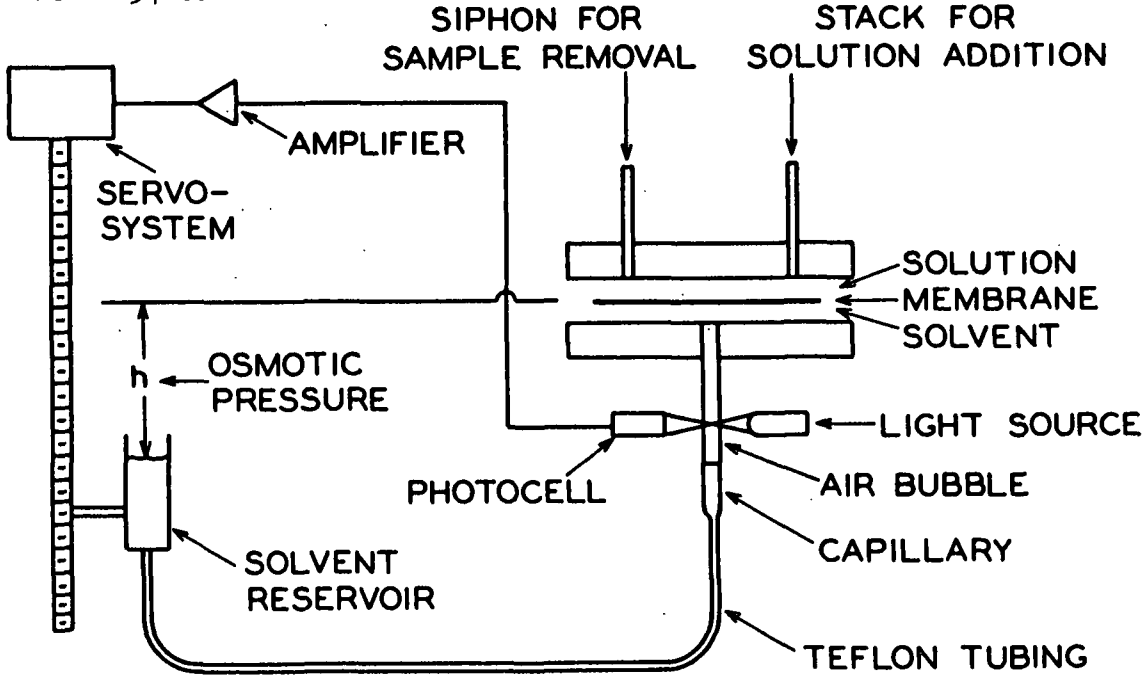

Figure 7. Schematic Diagram of Mechrolab High-Speed Membrane Osmometer, Model 501

The design of the instrument is such that, with an organic solvent and a UA .07 cellulose membrane ("very dense," Schleicher and Schuell Company, Keene, New Hampshire), osmotic pressures are readable and reproducible to ± 0.01 cm. of solvent in 3 to 15 min., thus holding to a minimum errors introduced by solute diffusion through the membrane.

The solution, approximately 1 ml., is introduced (see Fig. 7) and displaces the solvent or previous sample on the solution side of the membrane. An optical transducer on the solvent side of the membrane detects as little as 10^{-9} liters of solvent flow toward the membrane. The detection is due to change in light scattering as the bubble enters the light path. The transducer then causes the servo-system to adjust the pressure on the solvent side, by adjusting the height of the solvent reservoir, to prevent solvent transfer through the membrane.

The osmotic pressure data were treated according to the equation (34, 40),

$$\pi/c = (\pi/c)_0 [1 + \Gamma_2 c] = RT/\bar{M}_n [1 + \Gamma_2 c] \qquad (11),$$

by plotting the reduced osmotic pressure, π/c, as a function of concentration, c, and extrapolating to zero concentration, as shown in Fig. 8. The number-average molecular weight, $\bar{M}_n$, and the osmotic second virial coefficient, Γ_2, were calculated according to Equation (11) from the intercept and slope, respectively.

The osmotic pressure measurements were made for a series of concentrations for each fraction. The solvent point was then re-established, and the measurements on the series of concentrations repeated. A least-squares fit of the duplicate measurements was used to calculate $\bar{M}_n$ and Γ_2. The same membrane was used for all the fractions. The results of the osmotic pressure measurements and calculations are given in Table VII.

LIGHT SCATTERING

The light-scattering measurements were made in nitroethane at 25°C. with a Brice-Phoenix Light Scattering Photometer (Series 1937) at a wavelength of 5461 A. The performance of the instrument had been checked previously with known

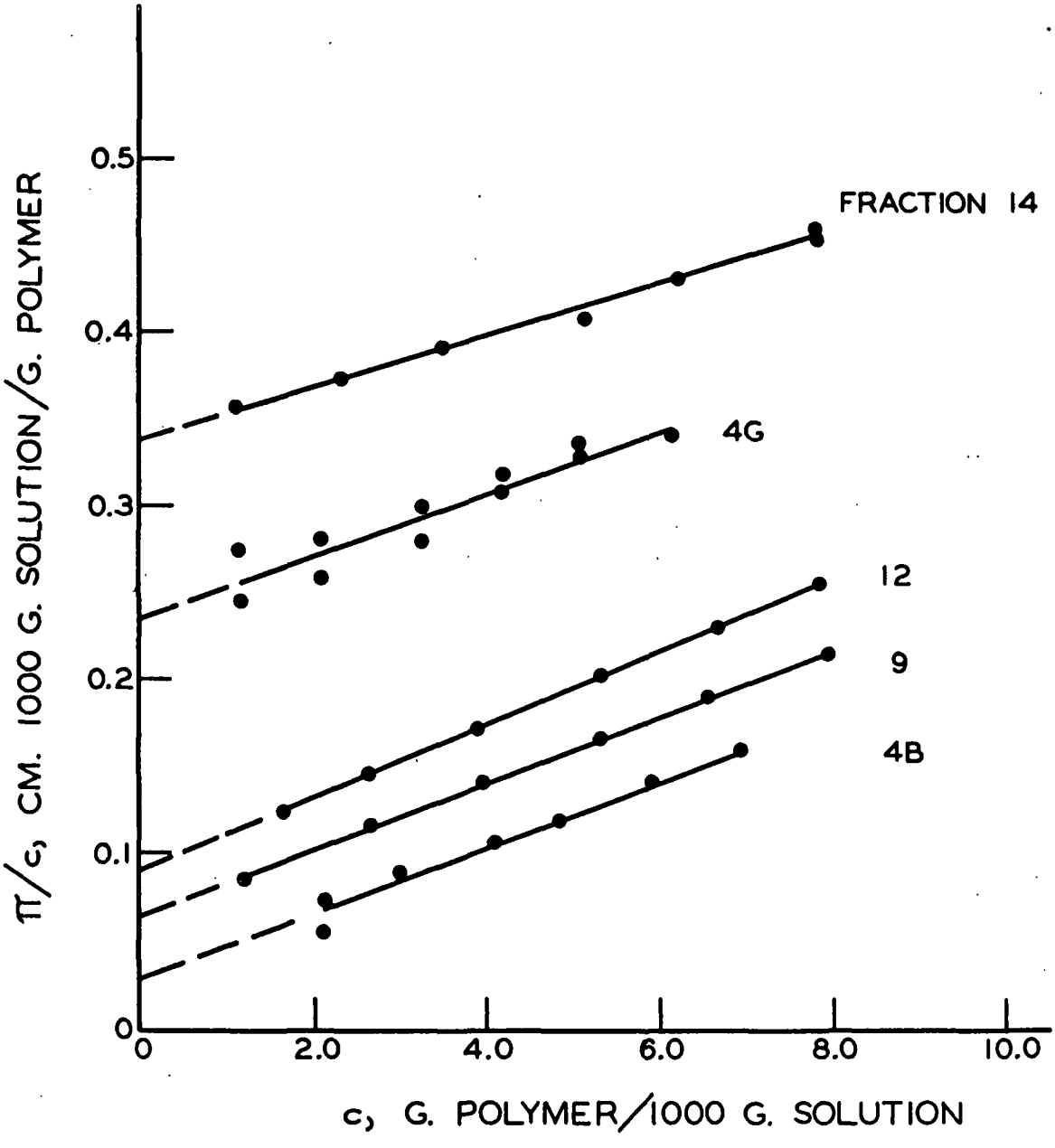

Figure 8. Reduced Osmotic Pressure as a Function of Concentration for Salep Glucomannan Triacetate in Nitroethane at 37°C.

samples of polystyrene in toluene (8). A small cylindrical cell (Brice-Phoenix C-101) was used for measurements of the angular dependence of scattering.

TABLE VII

RESULTS OF OSMOTIC PRESSURE MEASUREMENTS OF SALEP GLUCOMANNAN TRIACETATE IN NITROETHANE AT 37°C.

Fraction	$\bar{M}_n$ x 10^{-5} g./mole	$\bar{N}_n$	Γ_2 ml. $g.^{-1}$
14	0.772	268	41.5
4G	1.11	385	73.3
13	2.01	698	141
12	2.87	996	220
4F	3.06	1060	187
11	3.38	1170	231
9	3.95	1370	273
10	4.18	1450	288
8	4.70	1630	349
4D	6.12	2120	450
4B	9.25	3210	640

The low molecular weight fractions were clarified by repeated pressure filtration through solvent-resistant cellulose filters (Gelman Instrument Company, Chelsea, Michigan) of 4500 A. pore size until a constant light-scattering dissymmetry coefficient was obtained. The high molecular weight fractions were clarified by filtration through a coarse sintered glass funnel followed by ultracentrifugation at 51,000 g for 45 min. in a Beckman Model L-2 preparative ultracentrifuge, using stainless steel cups in a swinging bucket rotor (SW39L).

The excess turbitidy, τ, defined as the apparent turbidity of the solution minus the apparent turbidity of the solvent, of a dilute solution of a polymer

with a weight-average molecular weight $\overline{M}_w$ may be expressed as a function of the angle of observation, θ, and concentration, c, by (34, 43, 44),

$$Hc/\tau = [1/\overline{M}_w P(\theta)] + 2A_2c + ... \quad (12),$$

where $P(\theta)$, the particle scattering factor, is a complex function of θ and molecular size (43-47), A_2 is the light-scattering second virial coefficient, and the constant H is defined by (48, 49),

$$H = 32\pi^2 n_o^2 (dn/dc)^2/3\lambda^4 N_A \quad (13),$$

where

n_o = refractive index of the solvent

dn/dc = refractive index gradient of the solution

λ = wavelength of light used

N_A = Avogadro's number

The refractive index gradient of unfractionated salep glucomannan triacetate in nitroethane at 25°C. was determined in a Baird-Rayleigh interferometer at a wavelength of 5461 A. The value of 0.0756 ± 0.0015 ml./g. was found to be independent of concentration by making measurements at several concentrations.

The refractive index gradients of solutions of Fractions 4B, 8, and 14 were determined from sedimentation velocity runs on the Spinco Model E Analytical Ultracentrifuge, using the Rayleigh optical system. The change in refractive index, Δn, from solvent to solution was calculated from the equation (50),

$$\Delta n = J \lambda/a \quad (14),$$

where J is the number of Rayleigh fringes, λ is the wavelength of light (5461 A.), and a is the cell thickness (1.204 cm.). The refractive index of dilute solutions

is a linear function of concentration, and if the concentration of the solutions is known, dn/dc may be determined from the change in refractive index.

The value of dn/dc for the three fractions was found to be 0.0763 $\pm$ 0.0019 ml./g., which agreed, within experimental error, with the value of 0.0756 ml./g. determined on the Baird-Rayleigh interferometer for the unfractionated polymer. Therefore, the average value of 0.0760 ml./g. was used in the calculation of the constant H from Equation (13).

For all but Fraction 14 the values of Hc/τ were plotted as a function of $\sin^2(\theta/2) + kc$ and extrapolated to zero angle and zero concentration in the manner proposed by Zimm (44), as shown in Fig. 9-19. At zero scattering angle, $\theta = 0$, $P(\theta) = 1$ and the intercept of the Zimm plot is,

$$(Hc/\tau)_{\theta=0,\ c=0} = 1/\overline{M}_w \qquad (15),$$

from which weight-average molecular weights were calculated. The second virial coefficients were obtained from the slope of the Zimm plot at zero scattering angle. The z-average mean square radius of gyration was calculated from the initial slope and intercept of the zero concentration line according to the relation,

$$(\overline{S_z^2})^{1/2} = [(\lambda'/\pi)(3/16)^{1/2}][\text{Slope/Intercept}]^{1/2} \qquad (16),$$

where λ' is the wavelength of light in the solution. Results of these calculations are given in Table VIII.

The angular dependence of Hc/τ for Fraction 14 was not large enough to obtain satisfactory Zimm plots. Therefore $\overline{M}_w$, A_2, and $(\overline{S_z^2})^{1/2}$ were determined using the dissymmetry technique (43) and dissymmetry tables (51, 52). For low molecular weight polysaccharides it is sometimes difficult to decide which molecular model

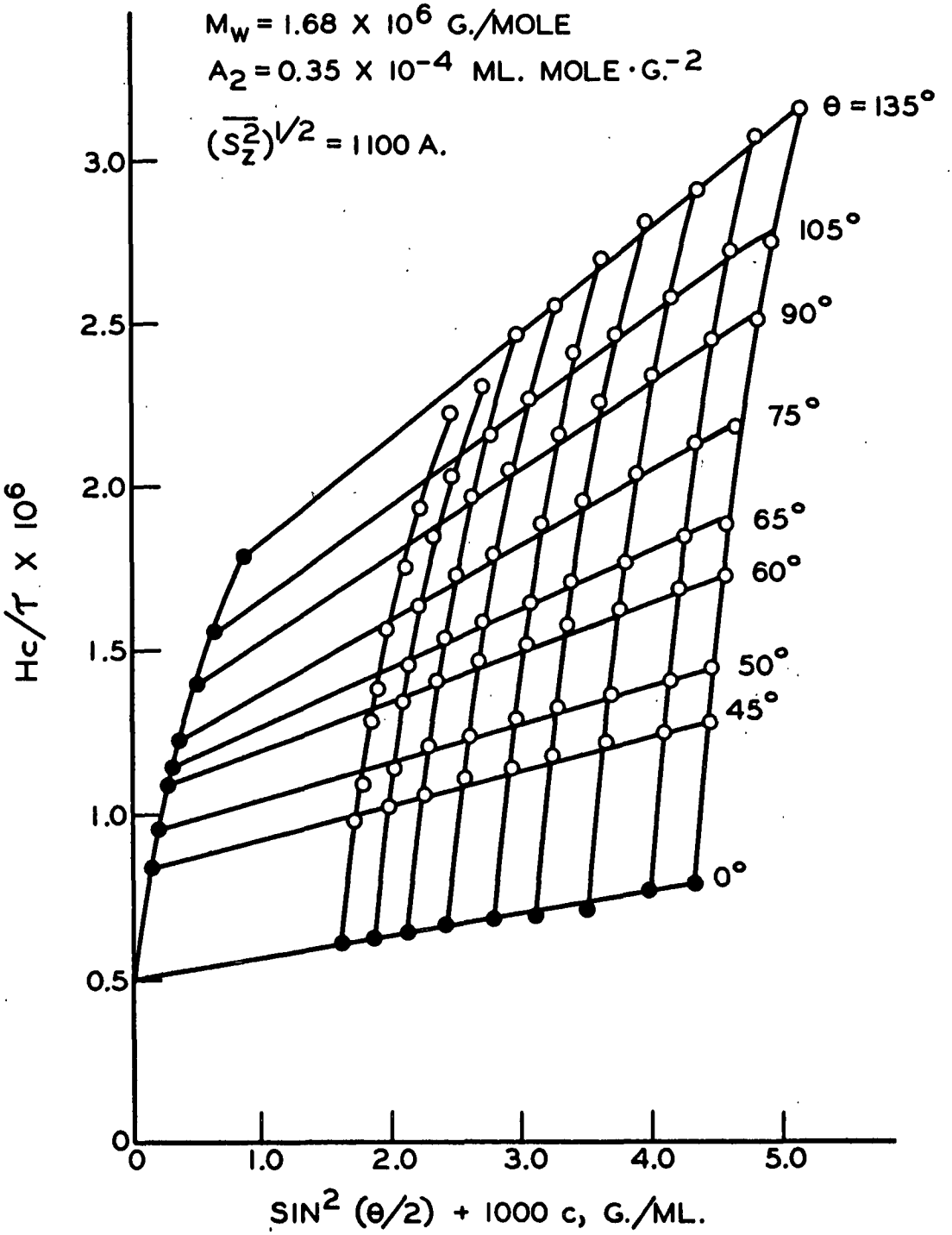

Figure 9. Zimm Plot for Salep Glucomannan Triacetate, Unfractionated, in Nitroethane at 25°C. λ = 5461 A.

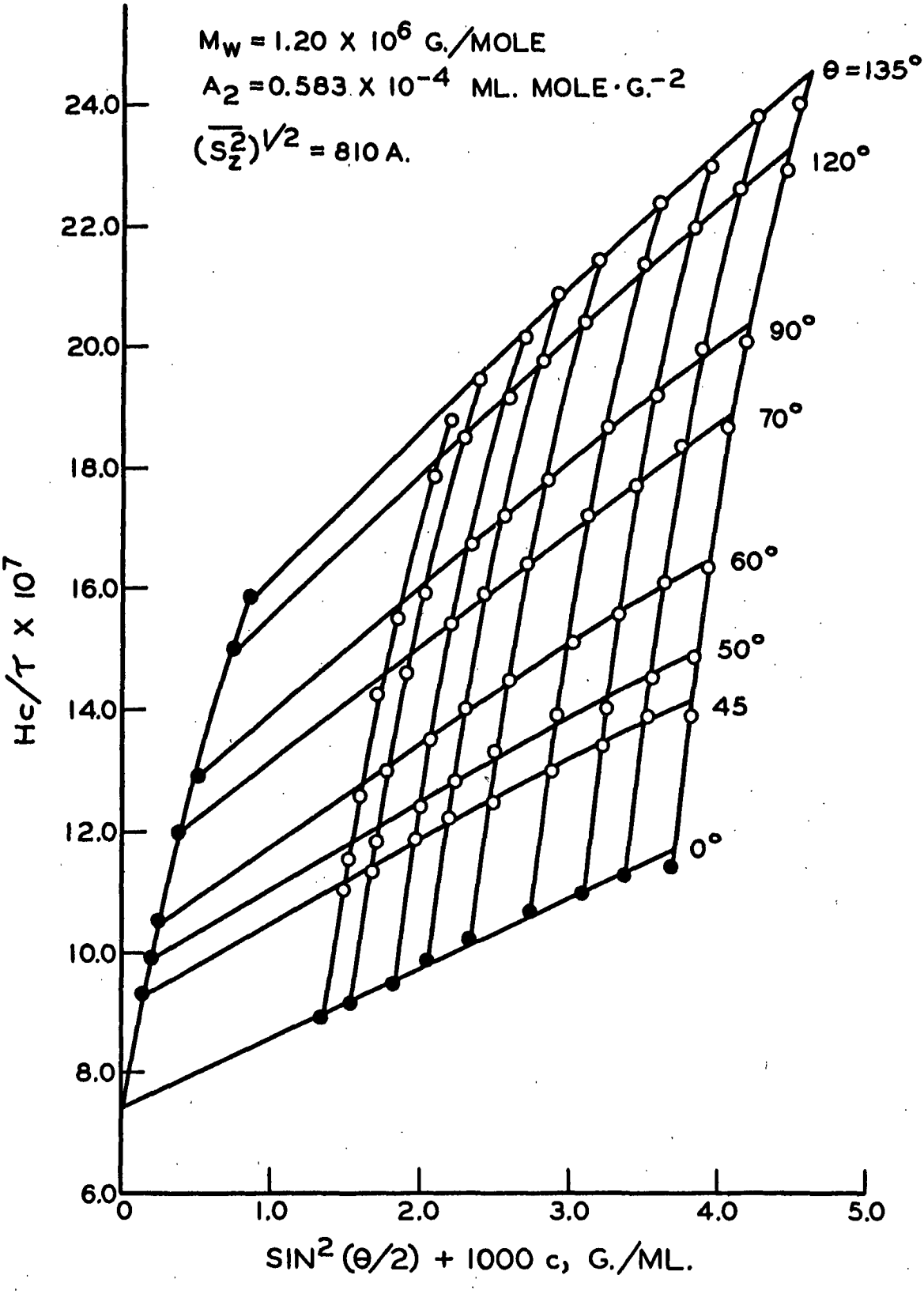

Figure 10. Zimm Plot for Salep Glucomannan Triacetate, Fraction 4B, in Nitroethane at 25°C. λ = 5461 A.

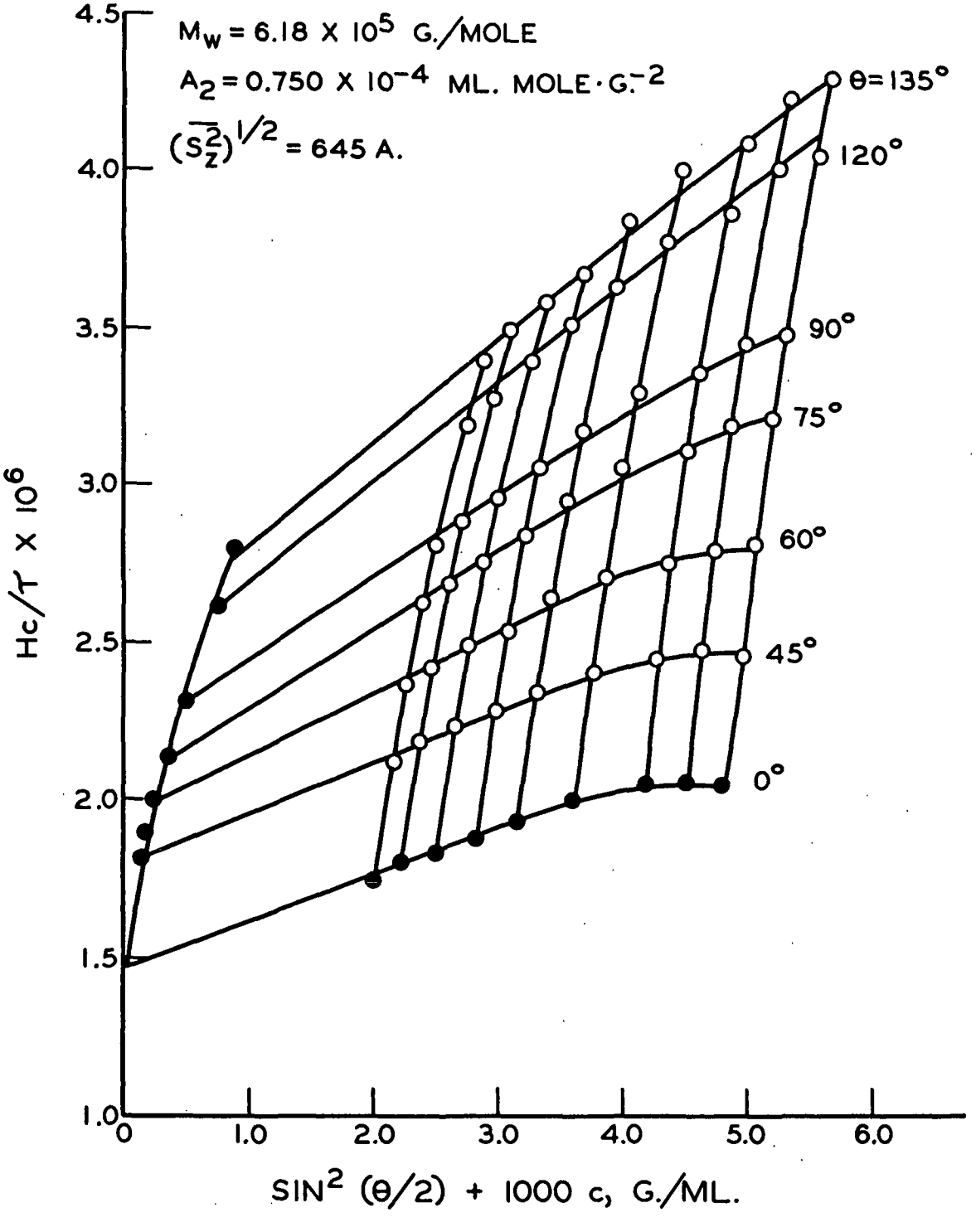

Figure 11. Zimm Plot for Salep Glucomannan Triacetate, Fraction 4D, in Nitroethane at 25°C. λ = 5461 A.

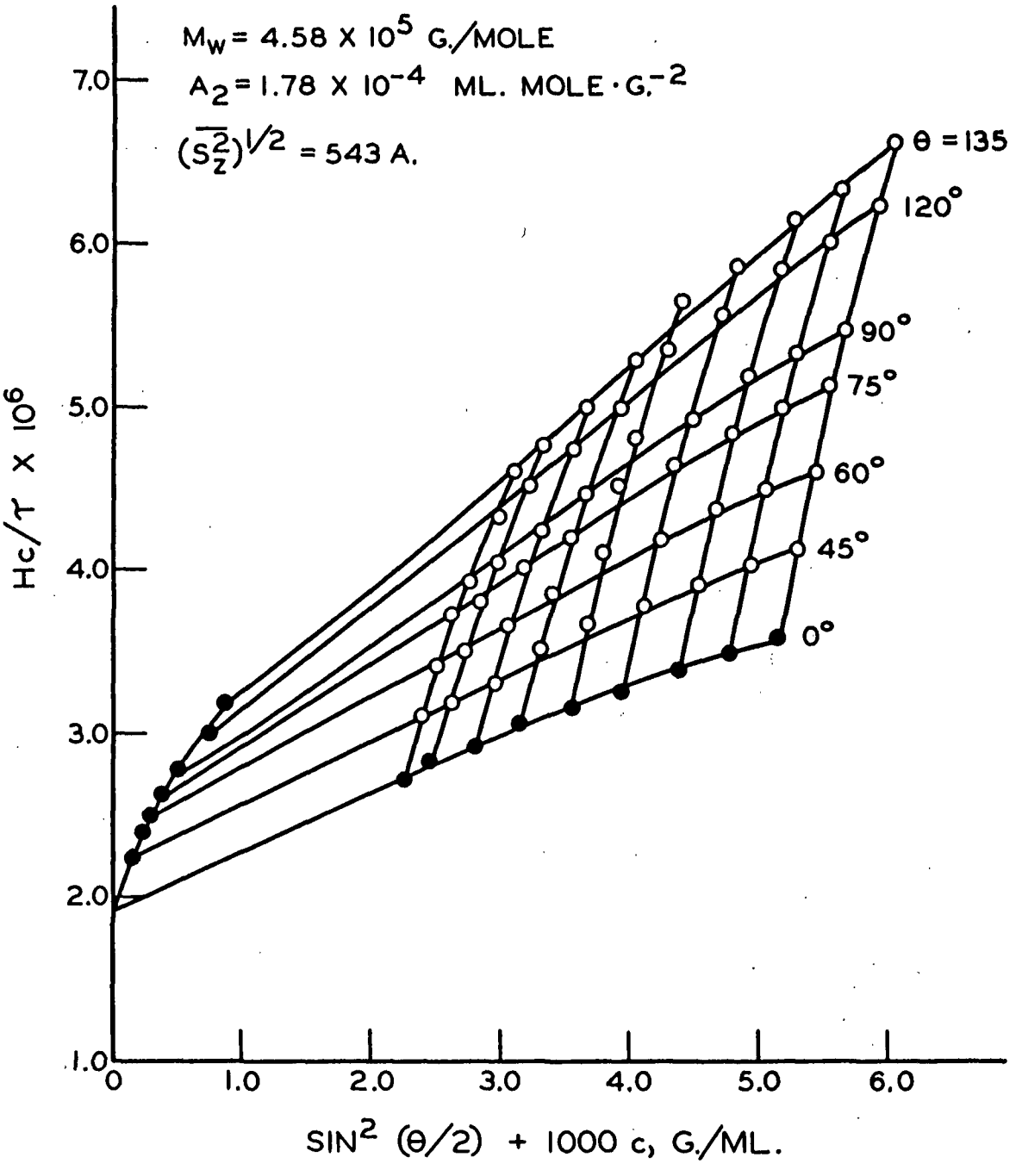

Figure 12. Zimm Plot for Salep Glucomannan Triacetate, Fraction 4E, in Nitroethane at 25°C. λ = 5461 A.

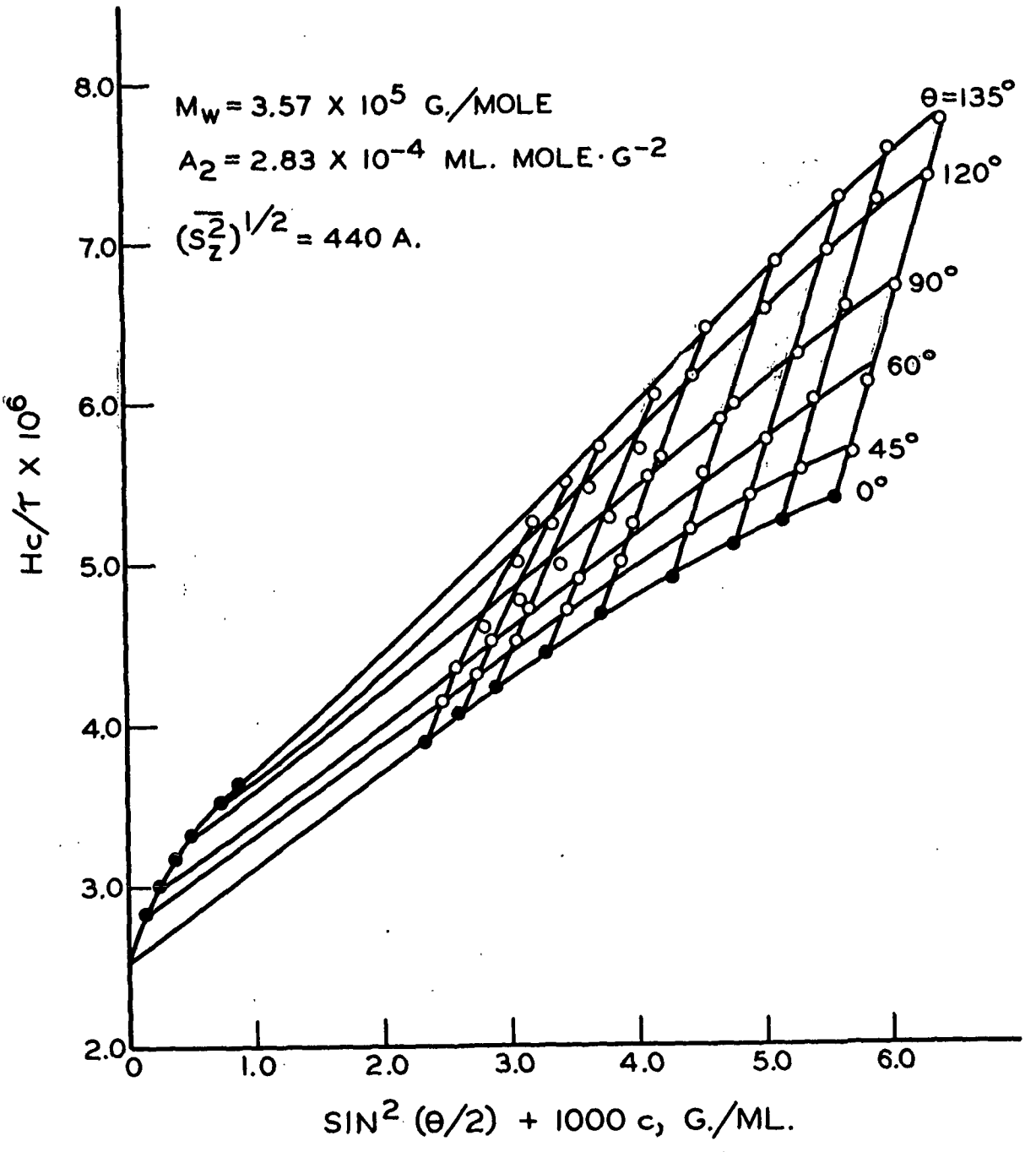

Figure 13. Zimm Plot for Salep Glucomannan Triacetate, Fraction 4F, in Nitroethane at 25°C. λ = 5461 A.

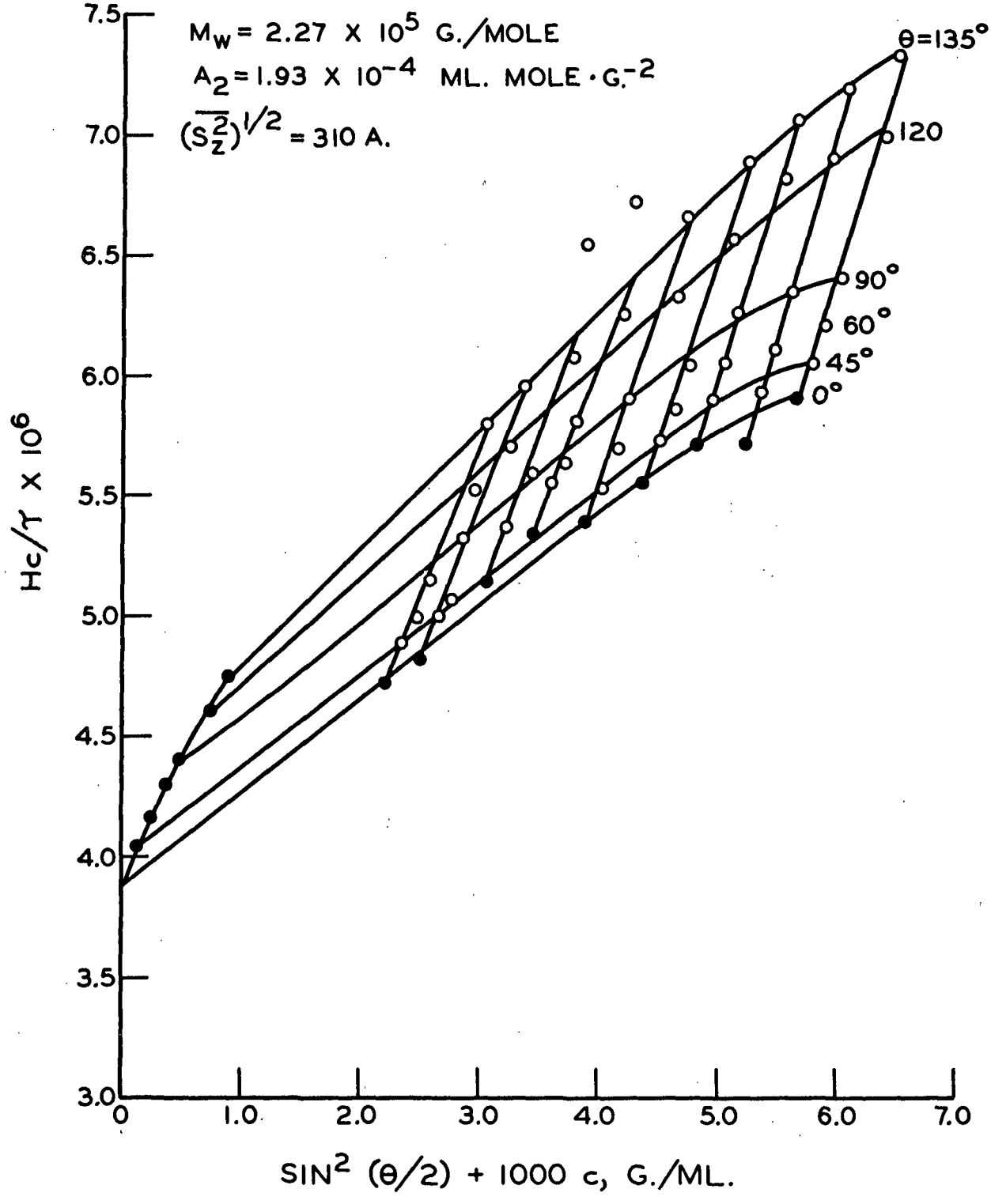

Figure 14. Zimm Plot for Salep Glucomannan Triacetate, Fraction 4G, in Nitroethane at 25°C. λ = 5461 A.

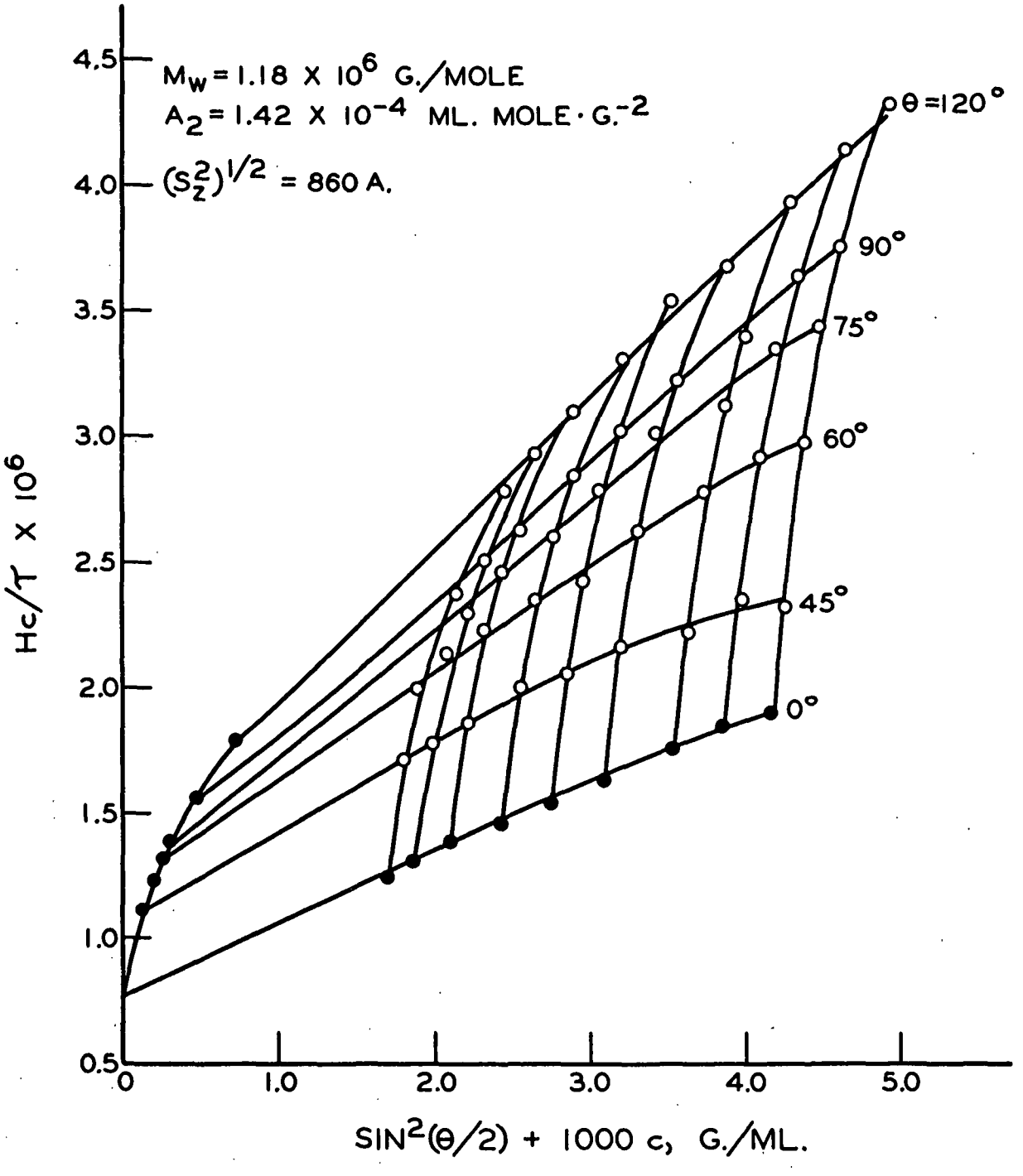

Figure 15. Zimm Plot for Salep Glucomannan Triacetate, Fraction 5, in Nitroethane at 25°C. λ = 5461 A.

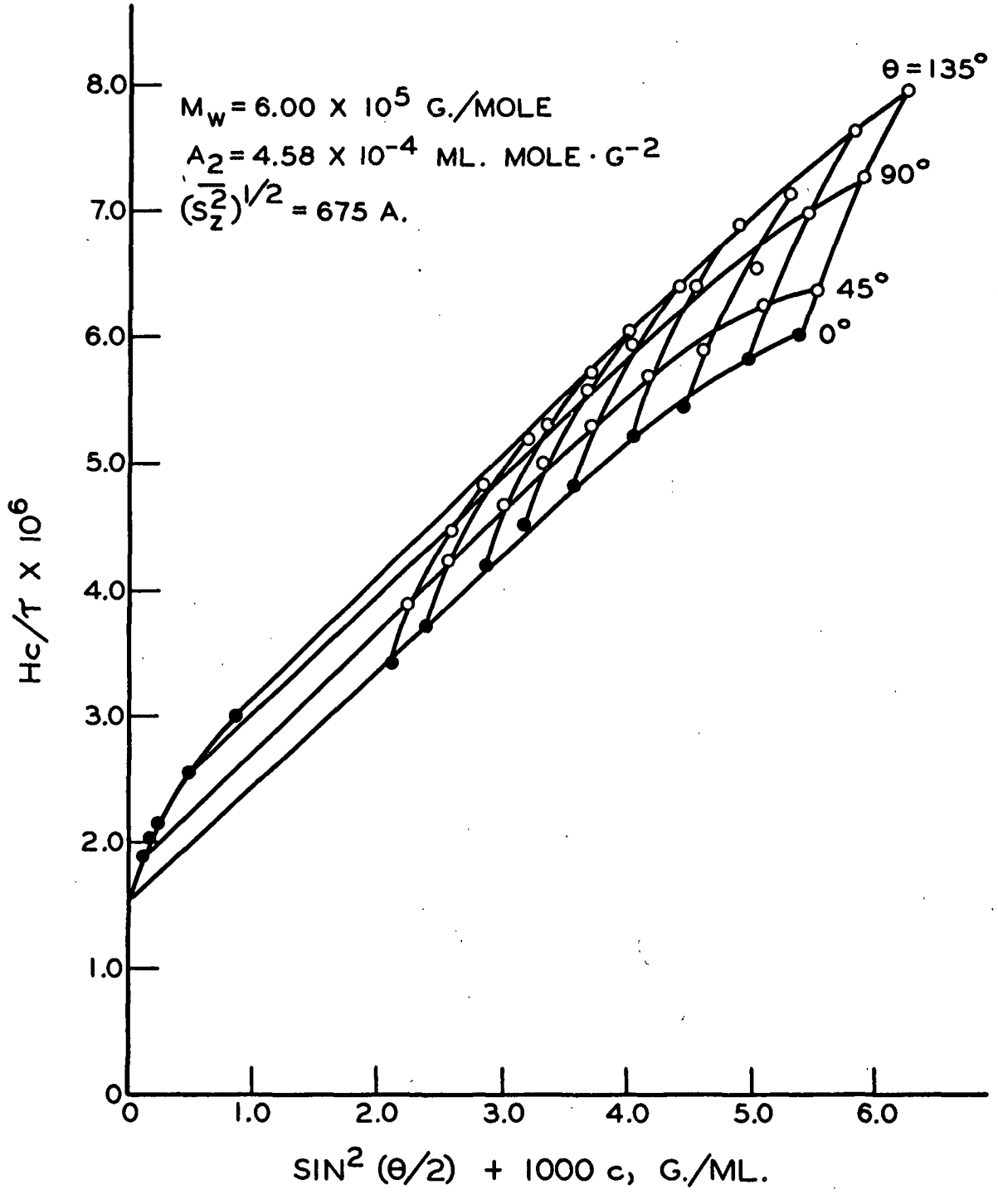

Figure 16. Zimm Plot for Salep Glucomannan Triacetate, Fraction 8, in Nitroethane at 25°C. λ = 5461 A.

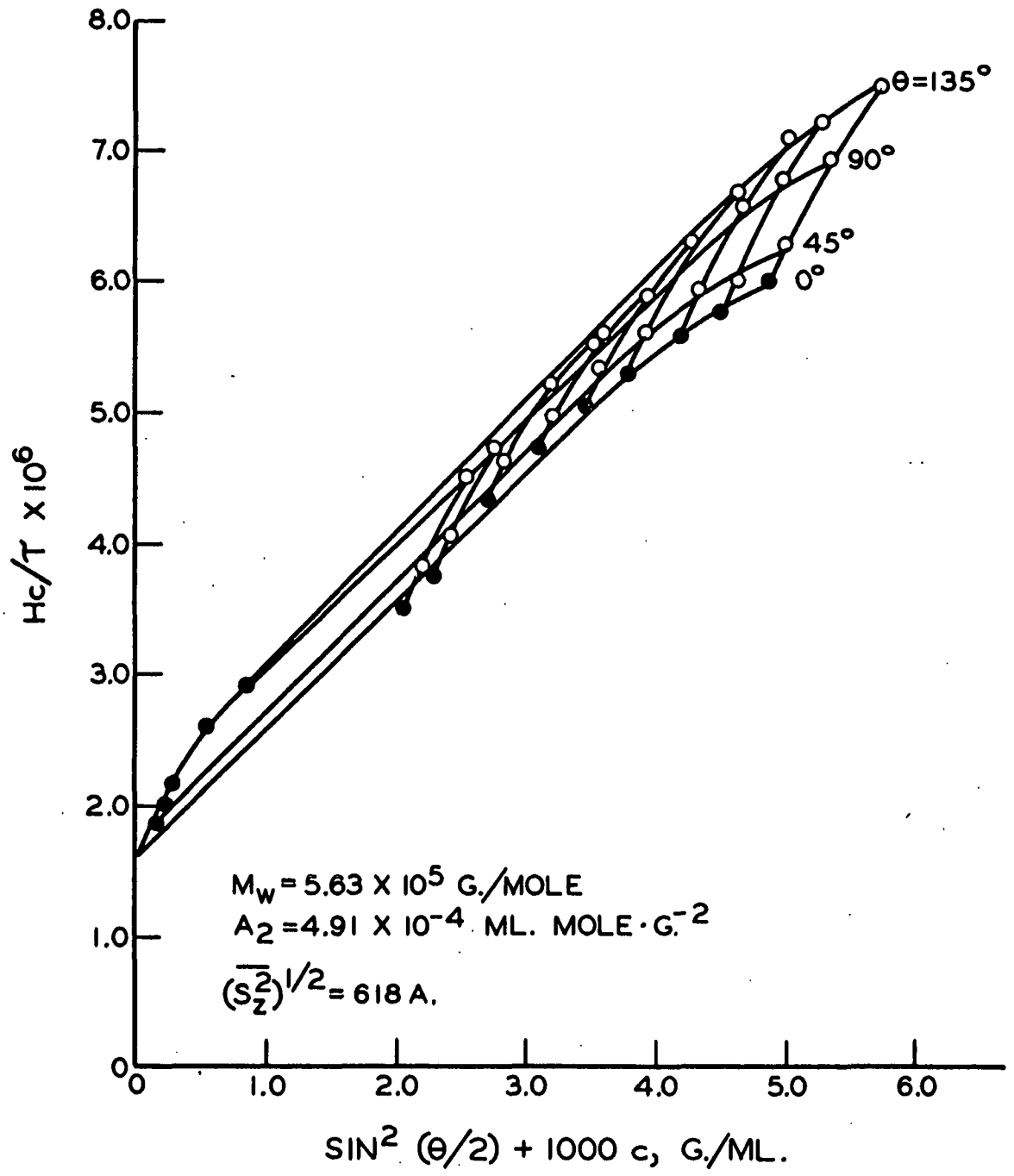

Figure 17. Zimm Plot for Salep Glucomannan Triacetate, Fraction 9, in Nitroethane at 25°C. λ = 5461 A.

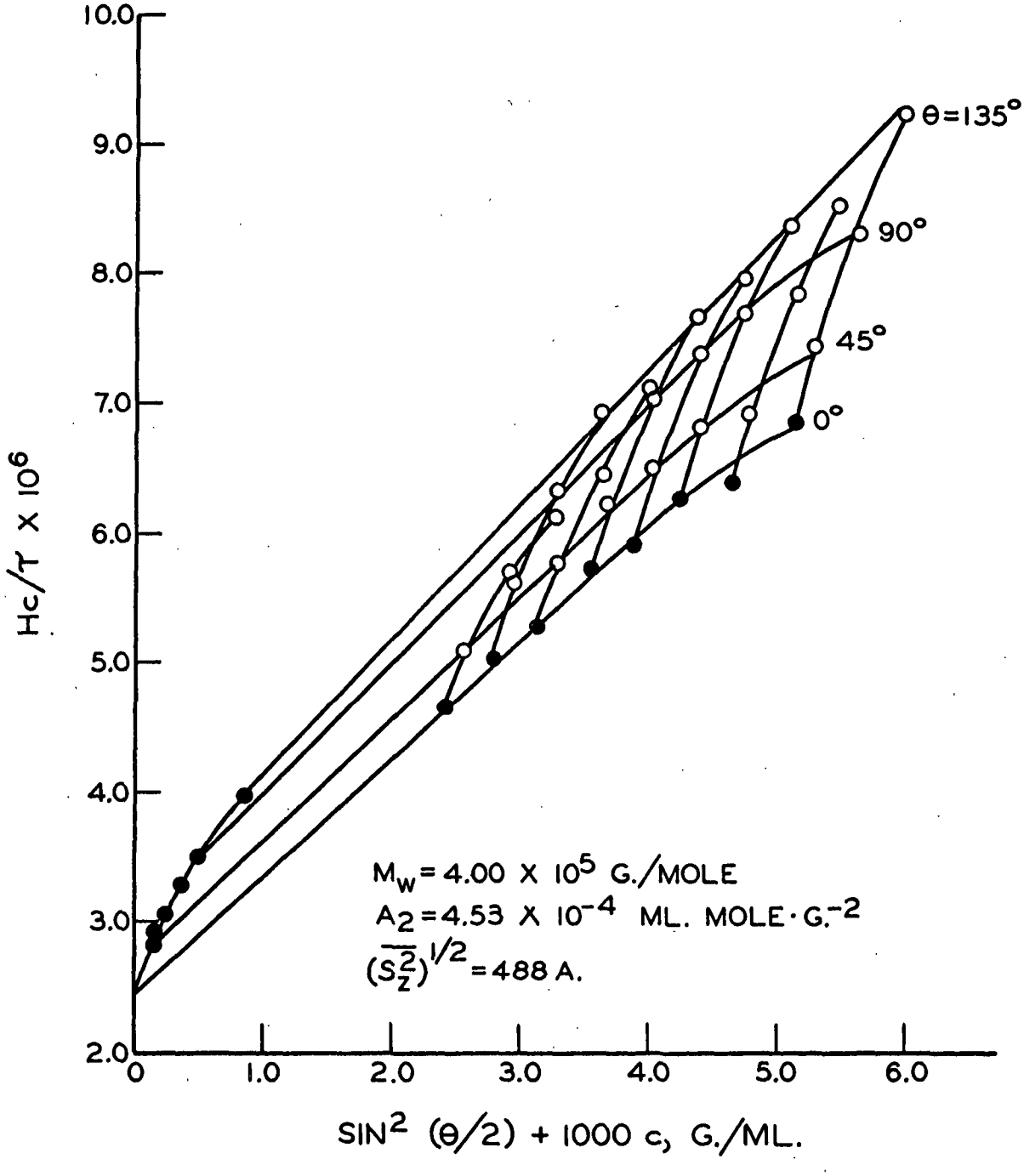

Figure 18. Zimm Plot for Salep Glucomannan Triacetate, Fraction 11, in Nitroethane at 25°C. λ = 5461 A.

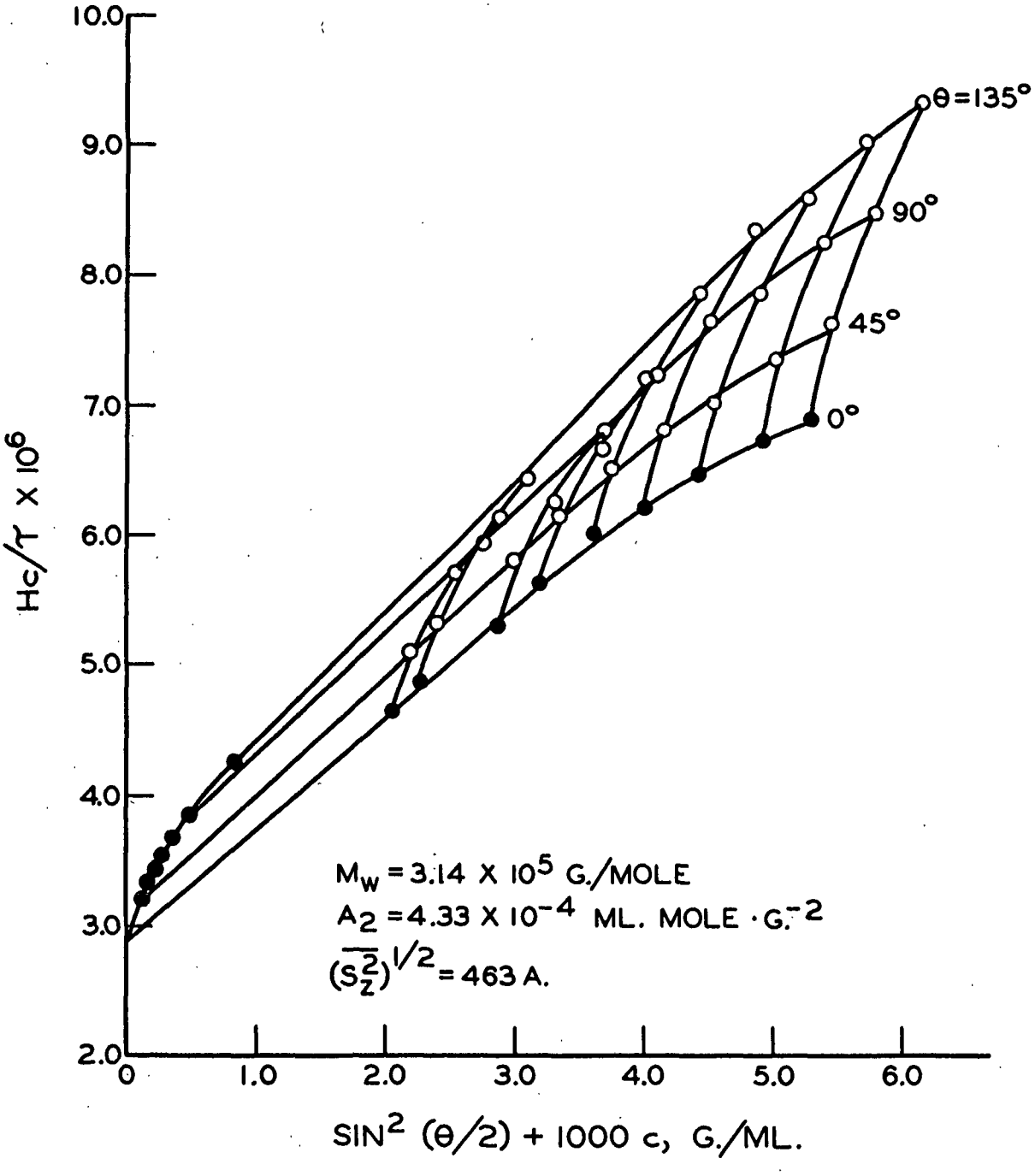

Figure 19. Zimm Plot for Salep Glucomannan Triacetate, Fraction 12, in Nitroethane at 25°C. λ = 5461 A.

TABLE VIII

RESULTS OF LIGHT-SCATTERING MEASUREMENTS OF SALEP GLUCOMANNAN TRIACETATE IN NITROETHANE AT 25°C.

Fraction Number	Cabannes Factor C_u	$\bar{M}_w \times 10^{-6}$, g./mole	$(D.P.)_w$	$(\overline{S_z^2})^{1/2}$, A.	$A_2 \times 10^4$, ml. mole g.$^{-2}$
Unfractionated	0.84	1.68	5830	1100	0.350
4B	0.89	1.20	4170	810	0.583
4D	0.90	0.618	2150	645	0.750
4E	0.88	0.453	1590	543	1.78
4F	0.90	0.357	1240	440	2.83
4G	0.88	0.227	789	310	1.93
5	0.88	1.18	4080	870	1.42
8	0.91	0.600	2080	675	4.58
9	0.87	0.543	1890	618	4.91
11	0.92	0.378	1310	488	4.63
12	0.92	0.325	1130	463	4.33
14	0.87	0.177	615	384[a] 402[b]	5.35

[a]This value was obtained by the dissymmetry method using the random coil model.

[b]This value was obtained by the dissymmetry method using the rigid rod model.

to use with the dissymmetry method. Therefore, results based on the random coil and rigid rod models are included in Table VIII.

The Cabannes depolarization factor (53, 54) correction was found to be 0.84 for the unfractionated polymer and 0.89 $\pm$ 0.03 for the fractions, as shown in Table VIII. The corrected molecular weights, given in Table VIII, were determined by multiplying the molecular weights determined from the Zimm plots or the dissymmetry technique by the Cabannes depolarization factor.

DISCUSSION

CHEMICAL COMPOSITION OF THE GLUCOMANNAN

The β-1,4-linked polysaccharide previously called salep mannan (10) has been shown in this study to be a β-1,4-linked glucomannan, which is in agreement with the findings of other workers (11-13). In this study, evidence for the linkage between glucose and mannose has been shown chromatographically by identification of the unknowns from a graded acid hydrolysis (19) of the glucomannan with authentic known samples of 4-O-β-D-glucosidomannose and 4-O-β-D-mannosidoglucose. The constant value of 2.7 for the ratio of mannose to glucose (M/G) when the glucomannan was fractionally precipitated by barium complex formation (24), and the agreement of this ratio with the value of 2.6 for the unfractionated polymer gave strong evidence that the polymer was a homogeneous glucomannan. The presence of O-acetyl groups (2%), as indicated by Husemann (10), was also shown.

Salep glucomannan is very similar to β-1,4-glucomannans from wood, having an M/G value identical with some of the latter (55). Its optical rotation of -44° in sodium hydroxide is in good agreement with that of some wood glucomannans. When the O-acetyl groups of salep glucomannan are removed it loses its water solubility, and this behavior has also been observed for the naturally acetylated glucomannans from wood (56). The outstanding difference between the glucomannans is the much higher molecular weight of salep glucomannan, and this is reflected in its much higher intrinsic viscosity.

It is not surprising that salep glucomannan has been thought to be a mannan. Prior to 1963, all of the studies of the chemical composition of the polymer had been done before the advent of paper chromatography. The establishment of the

composition of the polymer was based on the ability to crystallize and identify hydrolysis products of the methylated (57) and unmethylated (58) polymer, and on the specific rotation of the oxalic acid hydrolyzate (59) of the polymer. The studies on the identification of crystalline hydrolysis products were inconclusive since quantitative yields of mannose derivatives were not obtained. The specific rotation study was also inconclusive since a blank was not run to account for hydrolysis losses. Finally, in studying the solution properties of salep "mannan," Husemann (10) compared its properties to spruce "mannan" which has since been shown to be a glucomannan.

TREATMENT OF EXPERIMENTAL DATA ACCORDING TO THE EIZNER-PTITSYN THEORY

In treating intrinsic viscosity data, Eizner and Ptitsyn rearrange Equation (2) to yield

$$2^{3/2}\,\Phi_o\,(b^3/M)\,(N/[\eta])\;X\;(N/\lambda) =$$

$$(2\pi/3)^{1/2}\,[45/32(3 - 2^{1/2})]\;b/\lambda\;r_o + 1/\lambda^{3/2}\;\Phi(\lambda,N)\;N^{1/2} \qquad (17).$$

The correct value of λ is obtained by a trial and error procedure. A value of $\underline{\lambda}_i$ is assumed and $2^{3/2}\,\Phi_o\,(\underline{b}^3/\underline{M})\,(\underline{N}/[\eta])\;X\;(\underline{N}/\underline{\lambda}_i)$ is plotted as a function of $\Phi(\lambda,\underline{N})\;\underline{N}^{1/2}$. A least-squares fit of the data yields a straight line, and Equation (17) takes the form $\underline{Y} = \underline{A} + \underline{B}\underline{X}$. The slope of the line is $1/\underline{\lambda}_f^{3/2}$ from which $\underline{\lambda}_f$ is calculated. This procedure is repeated by assuming other values of $\underline{\lambda}_i$ and obtaining the corresponding $\underline{\lambda}_f$ values. The correct value of λ is obtained from the intersection of a line relating $\underline{\lambda}_i$ to $\underline{\lambda}_f$ with the straight line $\underline{\lambda}_i = \underline{\lambda}_f$. Then, using the correct value of λ, Equation (17) is plotted in the form $\underline{Y} = \underline{A} + \underline{B}\underline{X}$, as shown in Fig. 20, and the hydrodynamic radius of the monomer unit, $\underline{r}_o$, is calculated from the intercept.

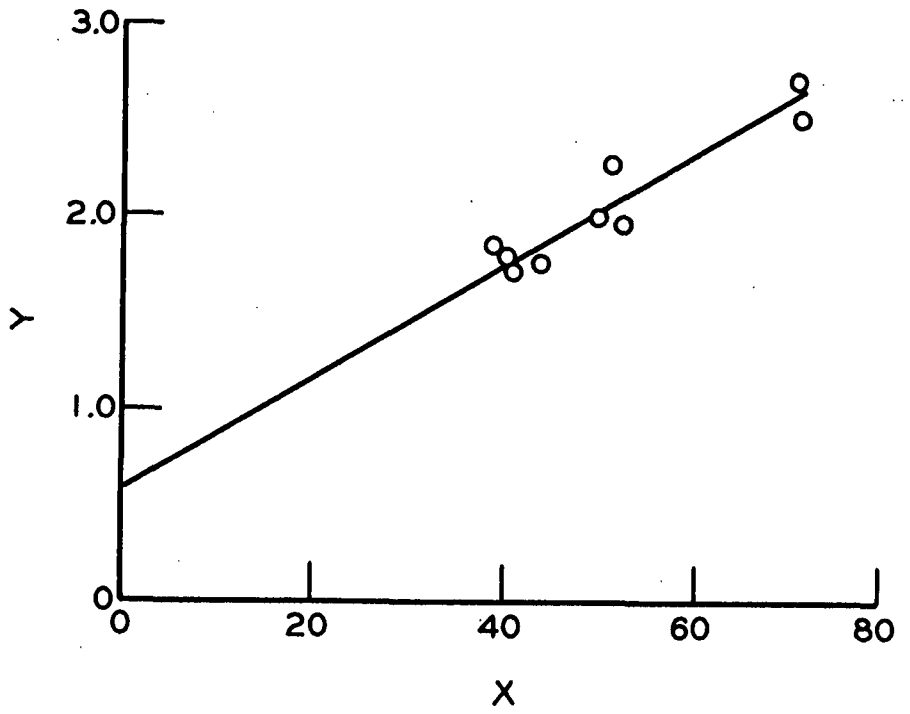

Figure 20. Intrinsic Viscosity Data for Salep Glucomannan Triacetate in Nitroethane According to the Eizner-Ptitsyn Theory. Open Circles and Straight Line Based on $\lambda = 10.7$ Calculated from $[\eta]$ - $\overline{N}_w$ Data

RESULTS

The Eizner-Ptitsyn treatment of intrinsic viscosity was made on the viscosity-molecular weight data for salep glucomannan triacetate, which is summarized in Table IX. Fractions 14 and 4G are much more polymolecular than the other fractions, probably because they were isolated by evaporating the fractional precipitation solutions, while the other fractions were isolated by fractional precipitation. Therefore, the Eizner-Ptitsyn treatment was carried out on the various fractions using $\overline{N}_w$ and $\overline{N}_\eta$, with and without Fractions 14 and 4G. The results are given in Table X. For comparison purposes the results of the Eizner-Ptitsyn treatment on cellulose acetate in acetone (60), guaran triacetate in acetonitrile (8), and cellulose nitrate in ethyl acetate (61) are included in the table.

TABLE IX

EXPERIMENTAL RESULTS OF VISCOSITY AND MOLECULAR WEIGHT MEASUREMENTS ON SALEP GLUCOMANNAN TRIACETATE IN NITROETHANE

Fraction Number	$[\eta]$, ml./g.	$\bar{N}_w$	$\bar{N}_n$	$\bar{N}_w/\bar{N}_n$
14	122	615	268	2.30
4G	152	789	385	2.04
13	182	--	698	--
12	228	1130	996	1.13
4F	263	1240	1060	1.17
11	295	1310	1170	1.12
4E	350	1590	--	--
9	365	1890	1370	1.38
10	362	--	1450	--
8	348	2080	1630	1.28
4D	428	2150	2120	1.01
4B	605	4170	3210	1.30
5	625	4080	--	--

RESULTS OF THE EIZNER-PTITSYN THEORY ANALYSES FOR SALEP GLUCOMANNAN TRIACETATE AND OTHER POLYMERS

Polymer	λ	Persistence Length, $\underline{a}$, A.	Hydrodynamic Monomer Radius, $\underline{r}_o$, A.	$\zeta/\eta_o=6\pi\underline{r}_o$, A.
Salep glucomannan triacetate				
Based on $\overline{N}_w$				
9 fractions[a]	10.7	55.1 ± 4	1.05 ± 0.3	19.8
11 fractions	12.9	66.4 ± 5	0.55 ± 0.2	10.4
Based on $\overline{N}_n$				
9 fractions[a]	12.7	65.4 ± 5	0.85 ± 0.3	16.0
11 fractions	10.1	52.0 ± 4	2.73 ± 1	51.5
Cellulose acetate				
Based on $\overline{N}_w$	11.5	59.3	9.87	186
Guaran triacetate				
Based on $\overline{N}_w$	11.2	57.8	3.04	57.3
Cellulose nitrate				
Based on $\overline{N}_w$	26.0	134	5.0	94.3

[a]Fractions 14 and 4G not used.

The values of $\underline{a}$ and $\underline{r}_o$ for salep glucomannan triacetate are different for the four sets of data. The persistence lengths, $\underline{a}$, based on $\overline{N}_w$ with and without Fractions 14 and 4G are 66.4 ± 5 and 55.1 ± 4 A., respectively; and based on $\overline{N}_n$ with and without Fractions 14 and 4G, the persistence lengths are 52.0 ± 4 and 65.4 ± 5 A., respectively. Therefore, these differences cannot be correlated to the polymolecularity of Fractions 14 and 4G. Figure 20 shows that there is considerable scatter in the data, to which differences in $\underline{a}$ and $\underline{r}_o$ must be attributed.

The variations in $\underline{a}$ for salep glucomannan triacetate are not very great and indicate only small differences in the configurational properties of the molecule.

This is particularly evident when one considers the persistence length of 134 A. for cellulose nitrate, which is less "flexible" than the acetate derivative of cellulose, and the persistence length of 8-10 A. for polystyrene (64), which is more "flexible" than cellulose derivatives. The persistence lengths of cellulose acetate, guaran triacetate, and salep glucomannan triacetate are nearly equal, indicating that the β-1,4-linked chains of D-glucose, D-mannose, or mixtures of D-glucose and D-mannose have similar configurations in spite of the structural differences of the anhydrosugar units.

The variations in $\underline{r}_o$ for salep glucomannan triacetate are more severe than those in $\underline{a}$. Assuming the Stokes equation, $\zeta/\eta_o = 6\pi\underline{r}_o$, to be valid for calculating the friction coefficient of a monomer unit, the various values of $\underline{r}_o$ will yield significantly different values of ζ/η_o, as shown in Table X. It is assumed that the length of the monomer unit of salep glucomannan triacetate, $\underline{b}$, is equal to that of cellulose (62) and guaran (63), since glucose and mannose would be expected to be in the C-1 conformation. Thus, with $\underline{b}$ being equal to 5.15 A., $\underline{r}_o$ should have a value approximately equal to $\underline{b}/2$, or 2.58 A. On this basis, the experimental $\underline{r}_o$ value of 2.73 A. appears to be the most reasonable. The other experimental values of $\underline{r}_o$ for salep glucomannan triacetate appear to be too small, and those for cellulose acetate and cellulose nitrate appear to be too large. The value of $\underline{r}_o$ as determined by the Eizner-Ptitsyn treatment is extremely sensitive to scatter in experimental data, which is probably the reason for the differences. Although the $\underline{r}_o$ values for the β-1,4-linked polysaccharides are quite different, they are more reasonable than values determined from other theories (9). In subsequent calculations the values used for $\underline{a}_1$ and $\underline{r}_o$ for $\overline{\underline{N}}_w$ and $\overline{\underline{N}}_n$ will be 55.1 A. and 1.05 A., and 52.0 A. and 2.73 A., respectively.

RADII OF GYRATION FOR SALEP GLUCOMANNAN TRIACETATE

The experimental values of the z-average root-mean-square radii of gyration, $(\overline{S^2_z})^{1/2}$, evaluated from light-scattering data according to Equation (16), are given in Table XI. These experimental values may be compared to the values calculated according to the Porod-Kratky "wormlike" model, used in the Eizner-Ptitsyn theory, from the following equation (45, 64):

$$(\overline{S^2_z})^{1/2} = a^2 \left\{ \overline{N}_z \, b/3a - 1 + (2a/\overline{N}_w b) \, [1 - (a/\overline{N}_n b)] \right\} \qquad (18).$$

In order to calculate the $\overline{N}_z$ for salep glucomannan triacetate fractions, the Zimm-Schulz type distribution (44) was assumed. According to this distribution, $\overline{N}_z$, $\overline{N}_w$, and $\overline{N}_n$ are expressed in terms of the Zimm-Schulz parameter, h, by,

$$\overline{N}_z/(h + 2) = \overline{N}_w/(h + 1) = \overline{N}_n/h \qquad (19).$$

The values of h and $\overline{N}_z$, calculated from the experimental values of $\overline{N}_w$ and $\overline{N}_n$, are given in Table XI.

Since $(\overline{S^2_z})^{1/2}$ was experimentally determined by light-scattering techniques, the persistence length of 55.1 A., evaluated by Eizner-Ptitsyn theory analysis from light-scattering molecular weight data, was used in Equation (18) to calculate the hydrodynamic values of $(\overline{S^2_z})^{1/2}$. The results, given in Table XI, show that the light scattering $(\overline{S^2_z})^{1/2}$ are approximately 30% higher than the hydrodynamic values. Because of the sensitivity of light scattering to dust particles at low angles, the error in the light scattering $(\overline{S^2_z})^{1/2}$ is ± 10%. The error in the determination of a is ± 7%. Therefore, the difference between the light scattering and hydrodynamic $(\overline{S^2_z})^{1/2}$ cannot be entirely explained by experimental error, and it becomes necessary to distinguish between the two. It is expected that the hydrodynamic radius of gyration should be different from the light-

TABLE XI

MOLECULAR PARAMETERS FOR SALEP GLUCOMANNAN TRIACETATE IN NITROETHANE

Fraction	$\bar{N}_z$	h	q_o	$(\overline{S_z^2})^{1/2}_{calcd.}$, A.[a]	$(\overline{S_z^2})^{1/2}_{exptl.}$, A.[b]	α	$(\overline{S_z^2})^{1/2}_{o}$, A.
14	967	0.0768	2.10	298	384	1.20	320
4G	1185	0.962	1.96	331	310	1.05	294
12	1250	7.70	1.18	340	463	1.16	400
4F	1420	5.89	1.24	363	440	1.08	410
11	1450	8.33	1.17	367	488	1.16	421
9	2410	2.63	1.50	476	618	1.18	524
8	2540	3.57	1.38	488	675	1.21	567
4D	2160	100.	1.00	450	645	1.02	636
4B	5130	3.33	1.42	696	810	1.02	791

[a] Calculated from Equation (18).

[b] Experimental values calculated from light-scattering data according to Equation (16).

scattering value, since the molecular properties being measured by the two methods are different. This behavior has been observed for other polysaccharides (8, 65).

CONFIGURATION OF SALEP GLUCOMANNAN TRIACETATE AND OTHER POLYMERS

To compare the configuration of salep glucomannan triacetate with other polymers it is convenient to consider the variable, $(\overline{S_z^2})_o^{1/2}/(r_{max})_z$, as a function of $(r_{max})_z$, as suggested by Swenson and Thompson (66). The unperturbed root-mean-square radius of gyration, $(\overline{S_z^2})_o$, is defined by,

$$(\overline{S_z^2}) = \alpha(\overline{S_z^2})_o^{1/2} \tag{20}$$

where $(\overline{S_z^2})^{1/2}$ is the experimentally determined value and α is the molecular expansion factor (34). For non-Gaussian coils with excluded volume effects, α may be calculated from experimental data by use of the equation (67, 68),

$$A_2 \bar{M}_w/[\eta] = 1.65\ [1 + 4.50\ (\alpha^2 - 1)] \tag{21}$$

where A_2 is the second virial coefficient. In a strict sense, this equation is not applicable to β-1,4-linked polysaccharides, since excluded volume effects are unimportant for these molecules. However, it is the only means of estimating α for the salep glucomannan triacetate – nitroethane system, and since α is small, the errors involved by using Equation (21) are only minor. The values of α, given in Table XI vary from 1.02 to 1.21, showing that the molecule is not greatly expanded by the solvent. This behavior has been found for other β-1,4-polysaccharides (8, 64, 65, 74).

In comparing the configuration of salep glucomannan triacetate with other polymers, log $[(\overline{S_z^2})_o^{1/2}/(r_{max})_z]$ is plotted as a function of log $(r_{max})_z$. This

was done in Fig. 21 for salep glucomannan triacetate in nitroethane at 25°C. (open circles); and guaran triacetate in acetonitrile at 22.5°C. (8), cellulose tricaproate in dimethylformamide at 41°C. and in 1-chloronaphthalene at 24°C. (69), and hydroxyethyl cellulose in water at 25°C. (65) [solid line]. The corresponding values for polystyrene in cyclohexane at 34°C. (70) [solid circles] are considerably below the polysaccharide curve, as would be expected for this more flexible molecular chain.

The similarity between guaran triacetate, hydroxyethyl cellulose, cellulose tricaproate, and salep glucomannan triacetate is quite evident and indicates that the molecules have a similar non-Gaussian behavior. This is consistent with the good agreement of the persistence lengths for salep glucomannan and guaran triacetate of 55.1 and 57.8 A., respectively.

THE β-1,4-POLYSACCHARIDE MODEL OF SALEP GLUCOMANNAN TRIACETATE

The Porod-Kratky persistence length is a useful parameter for characterizing the polymer chain but has the disadvantage that it does not specifically take into account the skeletal parameters of the chain.

According to Benoit (71) the cellulose chain may be represented by a series of parallel and perpendicular lines, as shown in Fig. 22. Salep glucomannan may also be represented by Benoit's model, since the bond lengths and structural conformations would be expected to be the same as those for cellulose. The vectors $\vec{a}_k/2 + \vec{b}_k + \vec{a}_k/2$ associated with the $a/2$ and b distances of the kth anhydroglucose unit (or anhydromannose) of the chain all lie in one plane. Values of $a/2 = 2.67$ A. and $b = 1.43$ A. have been calculated by Burchard (75). Internal rotation, restricted to the ether linkages, is described by the angle

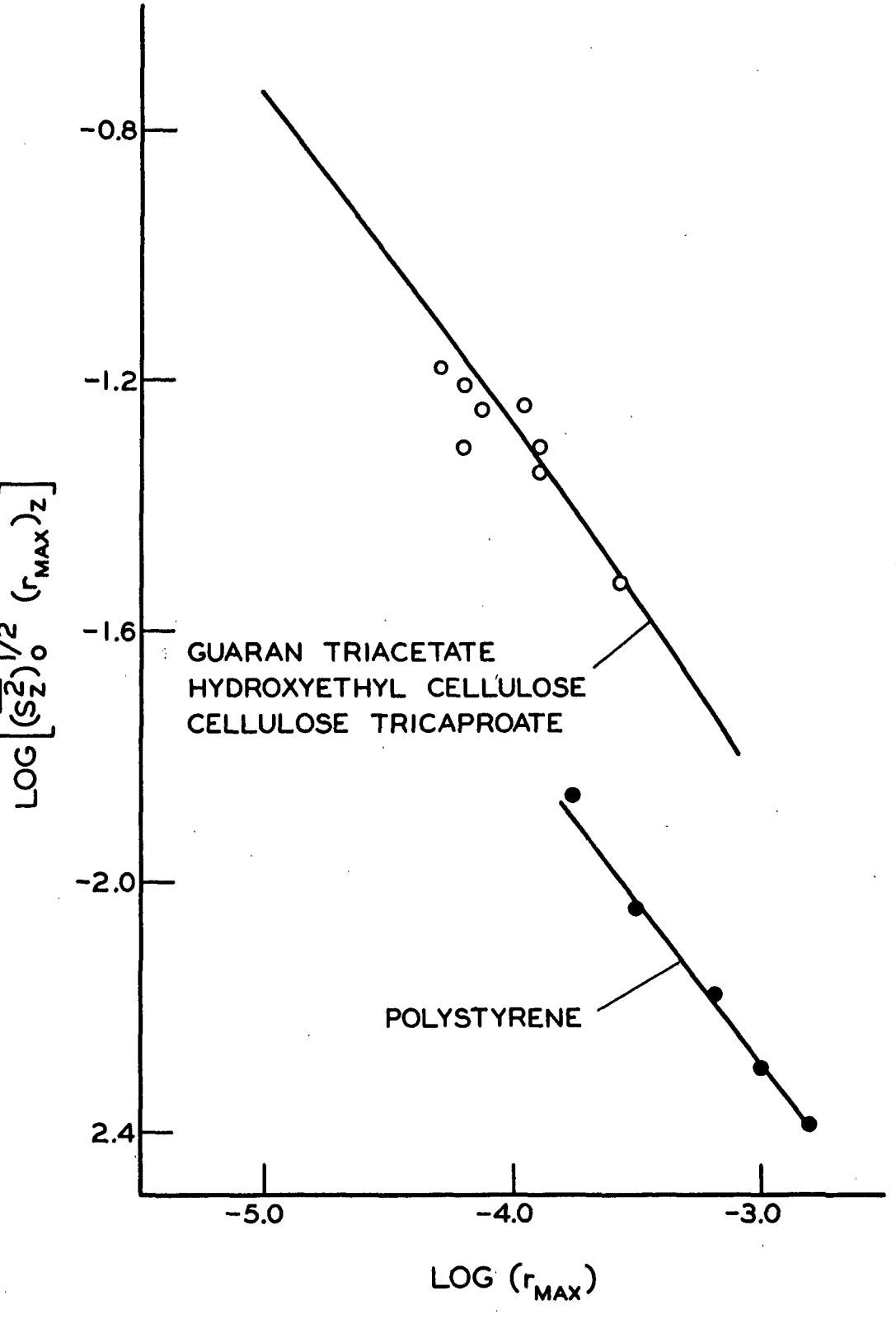

Figure 21. Dependence of $\log[(\overline{S_z^2})_o^{1/2}/(r_{max})_z]$ on $\log (r_{max})_z$ for Salep Glucomannan Triacetate in Nitroethane (Open Circles) and Other Polymers. $(\overline{S_z^2})_o^{1/2}$ Determined by Light Scattering

ϕ_k which may vary between the limits $\pm\pi$ depending on the position of the vectors $\vec{a}_{k-1}/2 + \vec{b}_{k-1} + \vec{a}_{k-1}/2$ and $\vec{a}_{k+1}/2 + \vec{b}_{k+1} + \vec{a}_{k+1}/2$.

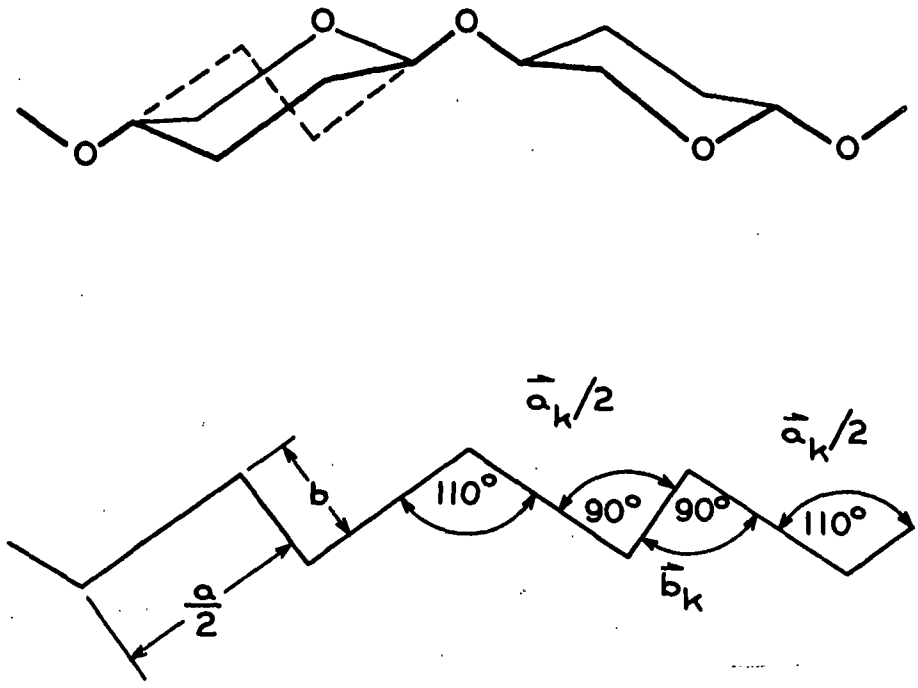

Figure 22. The Repeating Unit of Salep Glucomannan and the Corresponding Bond and Vector Diagram

Burchard and Husemann (72) have given expressions that relate the mean-square radius of gyration of a linear polymer to its chain dimensions, bond angles, and internal rotation angles. They point out that in the β-1,4-linked polysaccharides each chain member is turned through 180° with respect to its nearest neighbor, and, therefore, two rotational potential minima should exist, one at $\phi = 0°$ and the other at $\phi = 180°$.

For a single potential minimum, Burchard and Husemann (72) give,

$$(\overline{S^2})_o = N/6\left[\frac{a^2(1 + \cos\theta)}{(1 - \cos\phi)} + b^2\right]\left(\frac{1 + \overline{\cos\phi}}{1 - \overline{\cos\phi}}\right) \qquad (22),$$

and for two potential minima,

$$(\overline{S^2})_o = (N/6)\,(1/2)\left[\frac{a^2(1+\cos\theta)}{(1-\cos\theta)} + b^2\right]\left[\frac{(1+\overline{\cos\phi})}{(1-\overline{\cos\phi})} + \frac{(1-\overline{\cos\phi})}{(1+\overline{\cos\phi})}\right] \quad (23)$$

where θ is the supplement of the valence angle of the glycosidic oxygen $180°-\theta = 110°$, $(\overline{S^2})_o$ is the unperturbed radius of gyration, and N is the degree of polymerization.

As previously noted, it is necessary to distinguish between hydrodynamic and light-scattering radii of gyration; therefore, values of $\overline{\cos\phi}$ were evaluated from Equations (22) and (23) for both sets of data and are shown in Table XII.

TABLE XII

VALUES OF $\overline{\cos\phi}$, A MEASURE OF STERIC HINDRANCE TO ROTATION, FOR SALEP GLUCOMANNAN TRIACETATE IN NITROETHANE AT 25°C.

		$\overline{\cos\phi}$			
		Based on Hydrodynamic $(\overline{S_z^2})$		Based on Light Scattering $(\overline{S_z^2})_o$	
Fraction	$\overline{N}_z$	Equation (22)	Equation (23)	Equation (22)	Equation (23)
14	967	0.80	0.90	0.82	0.91
4G	1185	0.80	0.90	0.76	0.91
12	1250	0.80	0.90	0.85	0.93
4F	1420	0.80	0.90	0.84	0.92
11	1450	0.80	0.90	0.85	0.92
9	2410	0.80	0.90	0.84	0.92
8	2540	0.80	0.90	0.85	0.92
4D	2160	0.80	0.90	0.90	0.94
4B	5130	0.80	0.90	0.85	0.92

The steric hindrance may be accounted for by allowing limited rotation through an average angle $\pm \bar{\phi}$ about the ether linkage (41). The approximation of Debye (73)

$$\overline{\cos \phi} = \sin \bar{\phi}/\bar{\phi} \qquad (24)$$

may be used to evaluate $\bar{\phi}$. Equation (24) was evaluated by trial and error for the various average values of $\overline{\cos \phi}$, and the results are summarized in Table XIII.

TABLE XIII

HINDERED ROTATION ANGLE, $\bar{\phi}$, FOR SALEP GLUCOMANNAN TRIACETATE IN NITROETHANE AT 25°C.

	$\overline{\cos \phi}$	$\bar{\phi}$, °
Based on hydrodynamic $(\overline{S_z^2})$		
Single potential model	0.80	65.0
Double potential model	0.90	46.0
Based on light scattering $(\overline{S_z^2})_o$		
Single potential model	0.85	56.0
Double potential model	0.92	40.6

Large values of $\overline{\cos \phi}$, as found for salep glucomannan triacetate, guaran triacetate (8), cellulose (74), and cellulose derivatives (65, 72), indicate that the molecule is hindered in such a manner as to produce a highly extended chain. Swenson and Thompson (66) point out that xylans, having the same conformation as cellulose with the exception that the carbon-6 is absent, are relatively less extended than the β-1,4-hexosans. Thus, it would seem that one of the major causes of the relatively large extension of the β-1,4-hexosans is the presence of the carbon-6 on the main chain units.

HYDRODYNAMIC PROPERTIES OF SALEP GLUCOMANNAN TRIACETATE

INTRINSIC VISCOSITY – DEGREE OF POLYMERIZATION RELATIONSHIPS

Having determined the persistence length, $\underline{a}$, and the hydrodynamic radius of the monomer unit, $\underline{r}_o$, it is possible to calculate the dependence of intrinsic viscosity on degree of polymerization from the Eizner-Ptitsyn theory, using Equation (17). Since the $\underline{r}_o$ values of 1.05 A. and 2.73 A. are considered the most reasonable, they were used with their corresponding values of λ to calculate the dependence of $[\eta]$ on $\underline{\bar{N}}_w$ and $\underline{\bar{N}}_n$, respectively. As shown in Fig. 23 and 24, good agreement is obtained between theory and experiment, except for the low molecular weight fractions 14 and 4G. The greater polymolecularity of these fractions (see Table IX) is probably the reason these experimental values do not comply with theory. For most polymer solutions with a given $[\eta]$, a polymolecular sample will have a larger $\underline{\bar{N}}_w$ and a smaller $\underline{\bar{N}}_n$ than a monomolecular sample (40). Therefore, if Fractions 14 and 4G were less polymolecular they would fall closer to the theoretical lines for both $\underline{\bar{N}}_w$ and $\underline{\bar{N}}_n$.

According to the Eizner-Ptitsyn theory the relationship between intrinsic viscosity and degree of polymerization is a complex function of chain rigidity and hydrodynamic permeation of the solvent into the molecule. To examine how these factors affect the $[\eta]$ - $\underline{N}$ relationship, Equation (17) may be written as follows:

$$[\eta] = 0.384\ \bar{N}\ X\ (N/\lambda)/[6.62/\lambda r_o + (1/\lambda^{3/2})\ \Phi(N,\lambda)N^{1/2}] \qquad (25)$$

The geometric factor, $\underline{X}\ (\underline{N}/\lambda)$, shown in Fig. 25, may be represented by

$$X\ (N/\lambda) = (3/b^2\lambda)\ (\overline{S^2})/N \qquad (26)$$

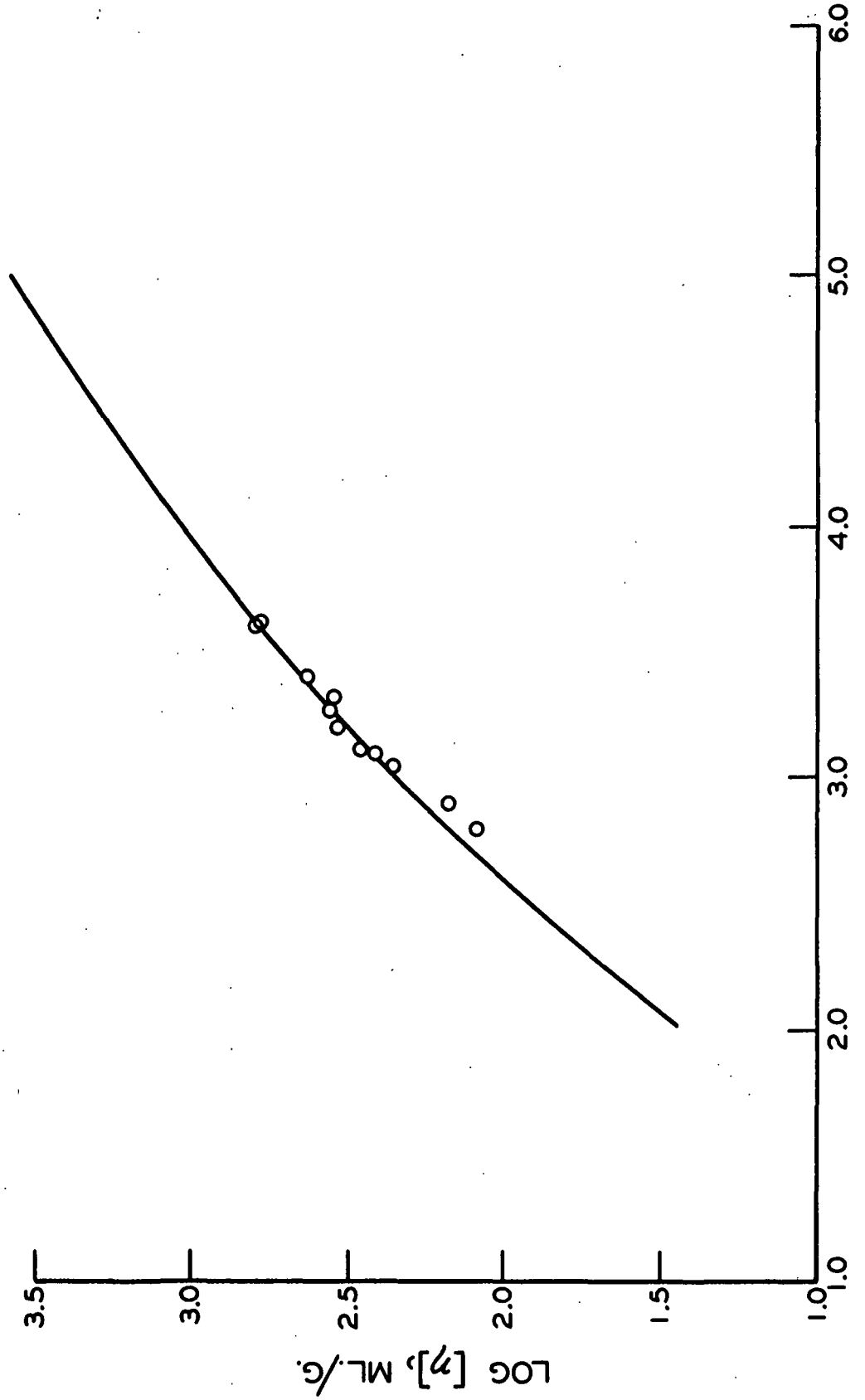

Figure 23. Intrinsic Viscosity as a Function of Weight Average Degree of Polymerization. Solid Line is the Theoretical Eizner-Ptitsyn Curve. The Open Circles are the Experimental Points

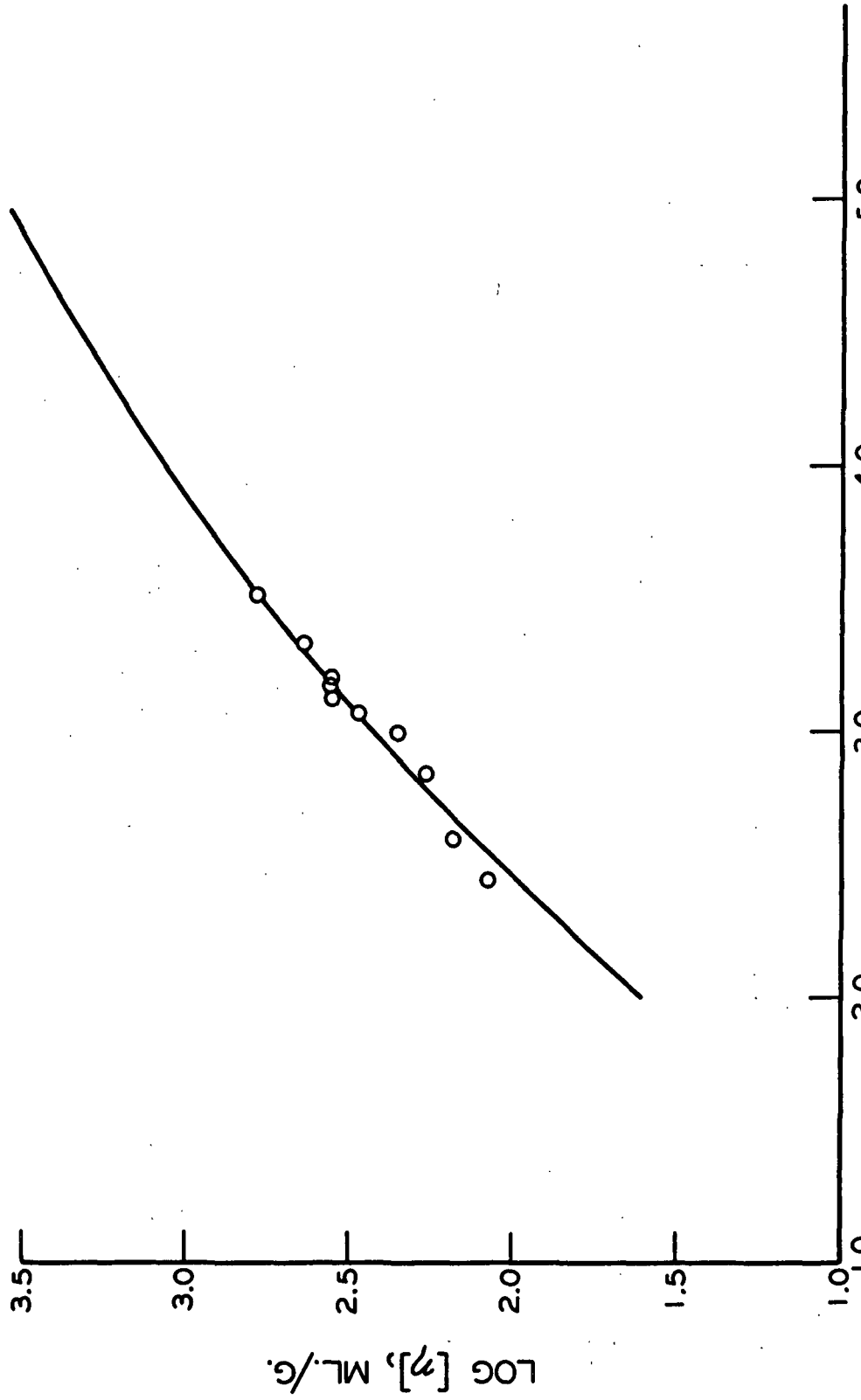

Figure 24. Intrinsic Viscosity as a Function of Number Average Degree of Polymerization. Solid Line is the Theoretical Eizner-Ptitsyn Curve. The Open Circles are the Experimental Points

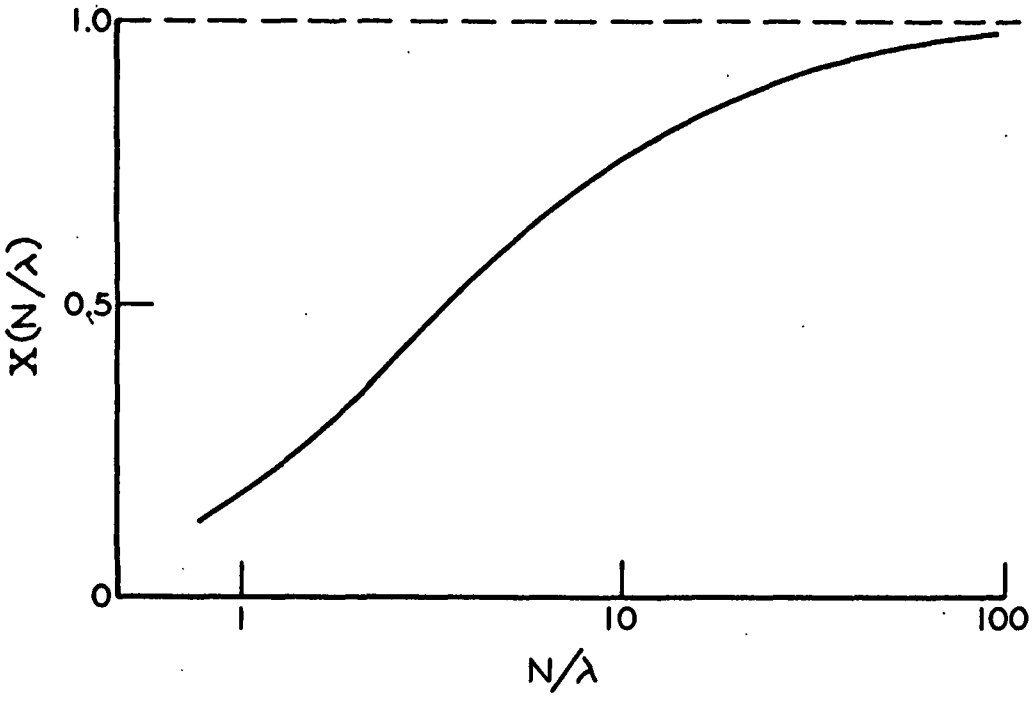

Figure 25. Eizner-Ptitsyn Geometric Factor as a Function of N/λ

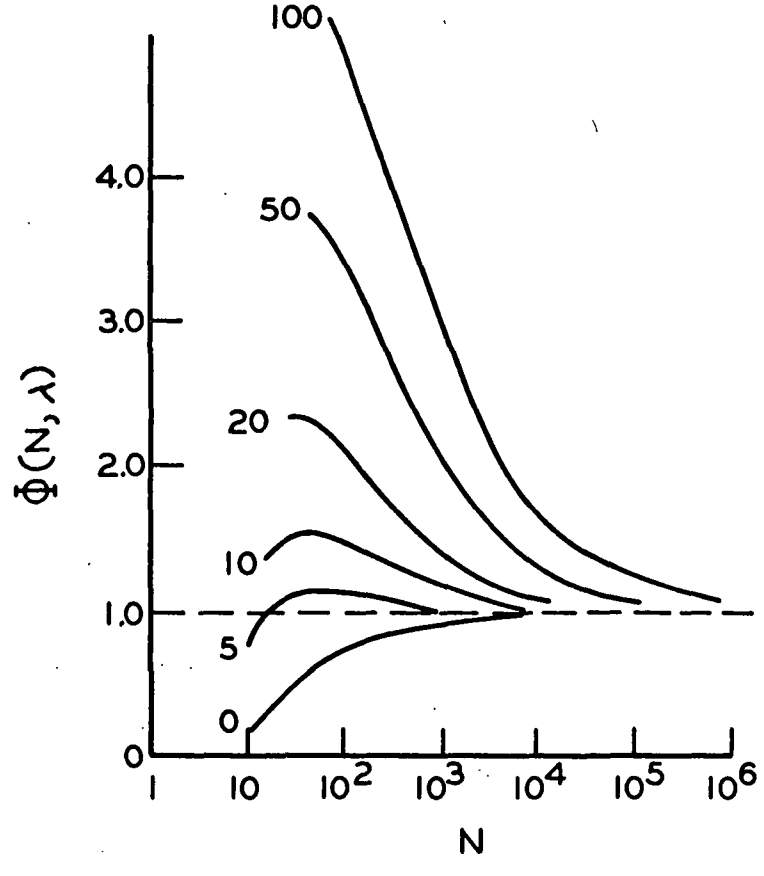

Figure 26. Eizner-Ptitsyn Hydrodynamic Function versus N

where $(\overline{S^2})$ is the mean-square radius of gyration. Since b and λ are constant, a change of $X(N/\lambda)$ reflects a change in $(\overline{S^2})/N$. As can be seen from Fig. 25 and Equation (25), at small values of N, $X(N/\lambda)$ changes with increasing N and serves to change the intrinsic viscosity – degree of polymerization relationship. At large values of N, $X(N/\lambda)$ reaches its limiting value of 1.0 and no longer influences the $[\eta]$ - N relationship.

The denominator of Equation (25) accounts for the change in the $[\eta]$ - N relationship due to the permeability of the solvent into the molecule. The first term in the denominator, a function of the persistence length and the monomeric friction coefficient, $\zeta = 6\pi r_o \eta_o$, is constant for a given polymer – solvent system. The second term includes the variable hydrodynamic function $\Phi(N,\lambda)$, shown in Fig. 26, and $N^{1/2}$. At low values of N, when permeability is significant, the first term of the denominator is more significant than the second. As N increases, the second term becomes more important; and finally at very large N, where permeability is no longer an important factor and $\Phi(N,\lambda) = 1$, the first term is negligible, $X(N/\lambda) = 1$, and $[\eta] \sim N^{1/2}$.

The above considerations may be used to discuss the $[\eta]$ - $\overline{N}$ relationships for salep glucomannan triacetate in nitroethane. The geometric factor, $X(N/\lambda)$, does not attain its limiting value over the range of molecular weights investigated, but it changes very slowly above $\overline{N} \cong 1000$. Therefore, over the entire experimental molecular weight range the change in the slope of the $[\eta]$ - $\overline{N}$ relationships is affected by two factors: a change in the geometric factor and a change in the hydrodynamic permeability. Above $\overline{N} \cong 1000$ the change in permeability is the main cause of the change in slope. Projecting to values of $\overline{N}$ above the maximum experimental values, log $[\eta]$ versus log $\overline{N}_n$ reaches its limiting slope of 0.5 at $\overline{N}_n \cong 10^5$, whereas log $[\eta]$ versus log $\overline{N}_w$ reaches the limiting

slope at $\bar{N}_w = 10^6$. This difference is caused by the larger value of r_o for the $\bar{N}_n$ data, which yields a smaller value of the first term in the denominator of Equation (25) for the $\bar{N}_n$ data than it does for the $\bar{N}_w$ data.

The hydrodynamic properties of guaran triacetate in acetonitrile (8) may be compared to those of salep glucomannan triacetate in nitroethane in light of the Eizner-Ptitsyn theory. The log $[\eta]$ versus log $\bar{N}_w = 5 \times 10^3$ compared with the projected value of $\bar{N}_w = 10^6$ for salep glucomannan triacetate. Since the λ values of salep glucomannan triacetate and guaran triacetate are nearly equal, the geometric factor influences the $[\eta]$ - $\bar{N}_w$ relationships to the same degree at equal values of $\bar{N}_w$. Therefore, the difference in log$[\eta]$ versus log $\bar{N}_w$ between salep glucomannan triacetate and guaran triacetate is caused by the difference in r_o, 1.05 A. and 3.04 A., respectively (see Table X), resulting in a smaller value of the first term in the denominator of Equation (25) for guaran triacetate than for salep glucomannan triacetate. If the difference in r_o is real, it can be concluded that the α-1,6-linked galactose side group causes the larger value of r_o for guaran triacetate. However, as previously stated, r_o is very sensitive to scatter in data, and the difference in r_o between salep glucomannan triacetate and guaran triacetate may be due to experimental error.

THE FLORY COEFFICIENT

According to Flory and Fox (6) the intrinsic viscosity may be represented by

$$[\eta] = \Phi_o (\overline{r_n^2})^{3/2} / \bar{M}_n \qquad (27)$$

where $(\overline{r_n^2})$ is the mean-square end-to-end separation of the polymer and Φ_o is a constant. For this equation to be valid it is necessary for the molecule to coil sufficiently so as to approach spherical symmetry, and for the internal hydrodynamic resistance to be great enough for Φ_o to approach its maximum value.

Since salep glucomannan triacetate does not satisfy these conditions, Φ will be used to distinguish the Flory coefficient from its maximum value, Φ_o. The value of Φ may be calculated from the Eizner-Ptitsyn theory by Equation (5) and from experimental data by the equation

$$\Phi = q_o [\eta] \bar{M}_w / 6(\overline{S_z^2})^{3/2} \qquad (28)$$

where q_o is a factor to correct for sample heterogeneity. Assuming the Zimm-Schulz type distribution (44), q_o may be calculated from the Zimm-Schulz parameter, h, by the equation,

$$q_o = (h + 2)^{3/2} \Gamma(h + 2)/(h + 1)^2 \Gamma(h + 1.5) \qquad (29).$$

The Zimm-Schulz parameters, q_o and h, for salep glucomannan triacetate are given in Table XI.

The Flory coefficient calculated from the Eizner-Ptitsyn theory, using 10.7 and 1.05 A. for λ and r_o, respectively, is shown as the solid line in Fig. 27. The values calculated from experimental data, corrected for heterogeneity, are given in Table XIV and also shown in Fig. 27.

When the hydrodynamic $(\overline{S_z^2})$ are used, good agreement is obtained between theory and experiment. This would be expected, since the hydrodynamic $(\overline{S_z^2})$ were calculated from the Porod-Kratky model, using the same λ used in calculating Φ from Equation (5). However, the agreement does show the ability to properly account for heterogeneity using the Zimm-Schulz distribution.

The light-scattering values of Φ are much lower than those predicted by the Eizner-Ptitsyn theory. This is also expected, since the light-scattering values of $(\overline{S_z^2})$ are approximately 30% greater than the hydrodynamic values.

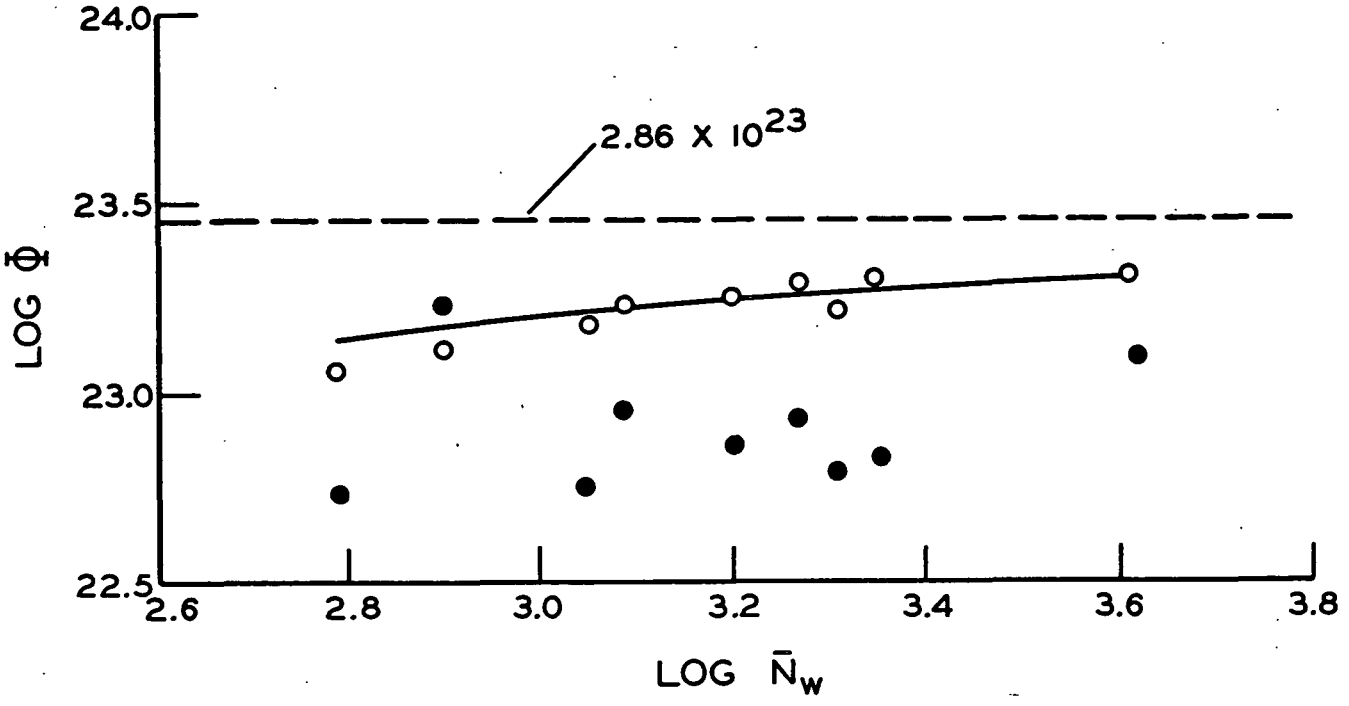

Figure 27. The Flory Coefficient as a Function of the Weight-Average Degree of Polymerization for Salep Glucomannan Triacetate in Nitroethane. The Solid Line is the Theoretical Eizner-Ptitsyn Curve. The Open Circles are Based on the Hydrodynamic $(\overline{S_z^2})$, and the Closed Circles are Based on the Light Scattering $(\overline{S_z^2})$

TABLE XIV

THE FLORY COEFFICIENT FOR SALEP GLUCOMANNAN TRIACETATE IN NITROETHANE

Fraction	$\Phi \times 10^{-23}$ Based on Hydrodynamic $(\underline{S^2_z})$	$\Phi \times 10^{-23}$ Based on Light Scattering $(\underline{S^2_z})$
14	1.14	0.55
4G	1.26	1.67
12	1.49	0.59
4F	1.66	0.92
11	1.79	0.76
9	1.87	0.86
8	1.67	0.64
4D	2.02	0.69
4B	2.08	1.33

The calculated values of Φ, being lower than Φ_o, show that salep glucomannan triacetate is not sufficiently coiled to have spherical symmetry and that the draining properties of the molecule are such that the internal resistance is not great enough for Φ to reach its maximum value, Φ_o. The increase in Φ with increasing $\underline{\overline{N}_w}$ implies that at a large enough value of $\underline{\overline{N}_w}$ the limiting conditions would be met. This is in agreement with the Eizner-Ptitsyn relationship between intrinsic viscosity and degree of polymerization.

CONCLUSIONS

It has been shown that the β-1,4-linked polysaccharide previously called salep mannan is a glucomannan with a mannose-to-glucose ratio of 2.6. The triacetate derivative has a weight-average degree of polymerization in the range of 615 to 4170, which is comparable to that of cellulose but much higher than the average value of 250 found for β-1,4-linked glucomannans from wood.

The dependence of the radius of gyration on the contour length of salep glucomannan triacetate is the same as that observed for cellulose tricaproate, hydroxyethyl cellulose, and guaran triacetate, indicating that β-1,4-linked chains of D-glucose, D-mannose, or mixtures of D-glucose and D-mannose have similar configurations in spite of the structural differences of the anhydrosugar units. The similarity of the configurations of salep glucomannan triacetate and guaran triacetate is also displayed in the nearly equal values of the persistence length of the Porod-Kratky chain model, as calculated from experimental data by the Eizner-Ptitsyn intrinsic viscosity theory.

Treatment of the intrinsic viscosity data according to the Eizner-Ptitsyn theory yields reasonable values of the monomeric friction coefficient, and indicates that the intrinsic viscosity – degree of polymerization relationship of salep glucomannan triacetate is affected over the entire molecular weight range by two factors: the partial permeability of the solvent into the molecule and the geometric factor, $\underline{X}\ (\underline{N}/\lambda)$. In comparison, the nondraining behavior of guaran triacetate is caused by its larger monomeric friction coefficient, and the fact that $\underline{N}$ is large enough so the $\underline{X}\ (\underline{N}/\lambda)$ reaches its limiting value of 1.0. Radii of gyration calculated from intrinsic viscosity and light scattering show that it is necessary to distinguish between the hydrodynamic and light-scattering radius of gyration.

The Flory coefficient, Φ, calculated from the Eizner-Ptitsyn theory, is lower than its limiting value and increases with increasing molecular weight. This behavior reflects the non-Gaussian configuration and the hydrodynamic permeability of salep glucomannan triacetate, and indicates that the molecule tends toward the limiting conditions of spherical symmetry and total internal resistance to flow. When the hydrodynamic radius of gyration is used, agreement with the theoretical Eizner-Ptitsyn values of Φ is obtained. Calculation of Φ from the light-scattering radius of gyration gives values which are lower than the theoretical values.

ACKNOWLEDGMENTS

I wish to thank The Institute of Paper Chemistry for the scholarship grant which made this thesis possible. To the many persons whose aid and advice helped in some way to the completion of this thesis, I also express my thanks. I especially wish to acknowledge the guidance and encouragement of my thesis advisory committee, Dr. S. F. Kurath, Mr. H. A. Swenson, and Mr. E. E. Dickey, and of Dr. L. E. Wise, who took an active interest in the progress of this thesis.

The aid of the following is gratefully acknowledged:

L. G. Borchert for analytical analyses;

J. J. Bachhuber and H. A. Swenson for the use of their IBM 1620 programs of the Eizner-Ptitsyn theory; and

J. A. Carlson for the operation of the ultracentrifuge.

A special thanks goes to my wife, Andrea, for her continual encouragement and her help in the mechanics of preparing this dissertation.

NOMENCLATURE

a	persistence length of the Porod-Kratky chain model
	dimension of a monomeric unit
	thickness of the double sector cell
$\vec{a}$	bond vector
A	constant in the Poiseuille equation
A_2	second virial coefficient from light scattering
b	dimension in a unit cell
	dimension of a monomeric unit
$\vec{b}$	bond vector
B	constant in the Poiseuille equation
c	concentration in weight per volume
C_u	Cabannes factor
dn/dc	specific refractive index gradient
g	gravitational constant
h	Zimm-Schulz parameter
	mean hydrostatic head in viscometry
H	constant in light-scattering equations
J	number of Rayleigh fringes
k	designation of monomer unit in polysaccharide model
	constant used to suitably spread concentration data on Zimm plot
k_1	constant relating concentration dependence of η_{sp}/c
k_2	constant relating concentration dependence of $(\ln \eta_{rel})/c$
L	length of a capillary tube in a viscometer
m_1	hydrostatic head from the top of a bulb in a viscometer
m_2	hydrostatic head from the bottom of a bulb in a viscometer

$\underline{M}$	molecular weight, subscript of n, w, or z indicates the number, weight, or z-average molecular weight, respectively
$\underline{M}_o$	molecular weight of a monomeric unit
$\underline{n}_o$	refractive index of the solvent
$\underline{N}$	degree of polymerization, subscript n, w, or z indicates the number, weight, or z-average degree of polymerization, respectively
	normality of chemical solutions
$\underline{N}_A$	Avogadro's number
$\underline{p}$	designation of a monomer unit in Peterlin intrinsic viscosity theory
$\underline{P}(\theta)$	particle scattering factor
$\underline{q}_o$	a correction term for polymolecularity
$(\underline{r}_n^2)$	number-average mean-square end-to-end distance
$(\underline{r}_{max})_z$	the z-average length of the fully extended polymer chain
$\underline{r}_{pt}$	distance between monomer units in the Peterlin intrinsic viscosity theory
$\underline{r}_o$	hydrodynamic radius of a monomer unit
$\underline{R}$	radius of capillary tube in a viscometer
	gas constant
$\underline{R}_f$	spot mobilities relative to the solvent front in paper chromatography
$\underline{R}_{gl}$	spot mobilities relative to glucose in paper chromatography
$(\overline{\underline{S}^2})$	mean-square radius of gyration. The subscript n, w, or z refers to number, weight, or z-average value, respectively
$(\overline{\underline{S}^2})^{1/2}$	root-mean square radius of gyration
$(\overline{\underline{S}^2})_o^{1/2}$	unperturbed root-mean square radius of gyration
$\underline{t}$	designation of a monomer unit in the Peterlin intrinsic viscosity theory
$\underline{T}$	absolute temperature
$\underline{X}$	fractional kinetic energy correction
$\underline{X}(\underline{N}/\lambda)$	geometric factor in Eizner-Ptitsyn theory

α	molecular expansion factor
	a designation of the mode of linkage between anhydrosugar units
$[\alpha]$	specific optical rotation
β	a designation of the mode of linkage between anhydrosugar units
Γ_2	second virial coefficient by osmometry
$\Gamma(\ )$	gamma function
$\Delta\underline{n}$	change in refractive index
ζ	friction coefficient of a monomer unit
η	viscosity of a liquid in the Poiseuille equation
η_o	viscosity of the solvent
$[\eta]$	intrinsic viscosity
η_{rel}	relative viscosity
η^*_{rel}	apparent relative viscosity
$\eta_{\underline{sp}}$	specific viscosity
$\eta_{\underline{sp}}/\underline{c}$	reduced viscosity
θ	scattering angle
	supplement of the fixed bond angle
λ	stiffness parameter in Eizner-Ptitsyn theory
π	3.1416 or osmotic pressure
$\pi/\underline{c}$	reduced osmotic pressure
ρ	density
τ	excess turbidity
$\tau_{\underline{R}}$	shear stress
$\emptyset$	angle between successive bond planes
Φ_o	Flory coefficient at its limiting value
Φ	Flory coefficient
$\Phi(\underline{N},\lambda)$	hydrodynamic function in Eizner-Ptitsyn theory

LITERATURE CITED

1. Debye, P., and Bueche, A. M., J. Chem. Phys. 16:573-9(1948).

2. Kirkwood, J. G., and Riseman, J., J. Chem. Phys. 16:565-73(1948).

3. Kurata, M., and Yamakawa, H., J. Chem. Phys. 28:785-91(1958).

4. Peterlin, A., J. Polymer Sci. 5:473-82(1950).

5. Kuhn, H., and Kuhn, W., J. Chem. Phys. 16:838-9(1948); J. Colloid Sci. 5:331-48(1950); J. Polymer Sci. 5:519-41(1950); 9:1-33(1952).

6. Flory, P. J., and Fox, T. G., Jr., J. Am. Chem. Soc. 73:1904-8(1951).

7. Eizner, Yu. E., and Ptitsyn, O. B., Vysokomol. Soedin. 4:1725-31(1962).

8. Koleske, J. V. The configuration and hydrodynamic properties of fully acetylated guaran. Doctor's Dissertation. Appleton, Wis., The Institute of Paper Chemistry, 1963. 175 p.; Koleske, J. V., and Kurath, S. F., J. Polymer Sci. Part A2:4123-49(1964).

9. Kurath, S. F., Schmitt, C. A., and Bachhuber, J. J., J. Polymer Sci. In press.

10. Husemann, E., J. prakt. Chem. 155:241-60(1940); C.A. 35:2321.

11. Daloul, M., Petek, F., and Courtois, J. E., Bull. Soc. Chim. Biol. 45:1247-54, 1255-60, 1261-6(1963).

12. Stepanenko, B. N., and Shcherbukhina, N. K., Biokhimiya 29:41-6(1964).

13. Slozhenikina, L. V., Shcherbukhina, N. K., and Stepanenko, B. N., Dokl. Akad. Nauk SSSR 153:960-3(1963).

14. Staudinger, H., and Heuer, W., Ber. 63:222(1930).

15. Kratky, O., and Porod, G., Rec. Trav. Chim. 68:1106(1949).

16. Peterlin, A., J. Chem. Phys. 33:1799-1802(1960).

17. Newman, S., Krigbaum, W. R., Laugier, C., and Flory, P. J., J. Polymer Sci. 14:451-62(1954).

18. Saeman, J. F., Moore, W. E., Mitchell, R. L., and Millett, M. A., Tappi 37:336-43(1954).

19. McKee, S. C. An investigation of the hydrolysis of a reduced 4-O-methyl-glucoronoxylan. Doctor's Dissertation. Appleton, Wis., The Institute of Paper Chemistry, 1961. 53 p.

20. Tyminski, A., and Timell, T. E., J. Am. Chem. Soc. 82:2823-7(1960).

21. Gyaw, M. O., and Timell, T. E., Can. J. Chem. 38:1957-66(1960).

22. Meier, H., Acta Chem. Scand. 14:749-56(1960).

23. Timell, T. E., Tappi 45:834-8(1962).

24. Meier, H., Acta Chem. Scand. 12:144-6(1958).

25. Vaughan, J. M. The oxidation of a spruce glucomannan with lead tetra-acetate. Doctor's Dissertation. Appleton, Wis., The Institute of Paper Chemistry, 1963. 65 p.

26. Thompson, N. A., Personal communication.

27. Institute Method 606 (modified).

28. Whistler, R., and Jeanes, A., Ind. Eng. Chem., Anal. Ed. 15:317-18(1943).

29. Carson, J. F., and Maclay, W. D., J. Am. Chem. Soc. 70:293-5(1948).

30. Genung, L. B., and Mallett, R. C., Ind. Eng. Chem., Anal. Ed. 13:369-74 (1941).

31. Weissberger, A., Proskauer, E. S., Riddick, J. A., and Toops, E. E., Jr. Techniques of organic chemistry. Vol. VII. 2nd ed. New York, Interscience, 1955. 552 p.

32. Scott, R. L., J. Chem. Phys. 13:178-87(1945); Ind. Eng. Chem. 45:2532-7 (1953).

33. Cregg, L. H., and Hammerschlag, H., Chem. Rev. 39:79-135(1946).

34. Flory, P. J. Principles of polymer chemistry. Ithaca, New York, Cornell University, 1953. 672 p.

35. Tompa, H. Polymer solutions. London, Butterworths, 1956.

36. Tanford, C. Physical chemistry of macromolecules. New York, John Wiley and Sons, Inc., 1961. 710 p.

37. Ubbelohde, L., Ind. Eng. Chem., Anal. Ed. 9:85-90(1937).

38. Schurz, J., and Immergut, E. H., J. Polymer Sci. 9:279-81(1952).

39. Hall, H. T., and Fuoss, R. M., J. Am. Chem. Soc. 73:265-9(1951).

40. Allen, P. W. Techniques of polymer characterization. London, Butterworths, 1959. 256 p.

41. Cowie, J. M. G., Makromol. Chem. 42:230-47(1961).

42. Mechrolab, Inc. Model 501 high-speed membrane osmometer. Operation manual. Mountain View, California.

43. Debye, P., J. Phys. and Colloid Chem. 51:18-32(1947).

44. Zimm, B. H., J. Chem. Phys. 16:1093-9, 1099-116(1948).

45. Benoit, H., and Doty, P., J. Phys. Chem. 57:958-63(1953).

46. Peterlin, A., J. Polymer Sci. 10:425-36(1953).

47. Stacey, K. A. Light scattering in physical chemistry. London, Butterworths, 1956. 230 p.

48. Brice, B. A., Hawler, M., and Speiser, R., J. Opt. Soc. Am. 40:768-78(1950).

49. Phoenix Precision Instrument Co. The new Brice Phoenix light scattering photometer. Operation manual OM-1000. Philadelphia, Pa., 1955. 52 p.

50. Beckman Instruments, Inc. Beckman Model E Analytical Ultracentrifuge, Instruction manual E-IM-3. Palo Alto, California, 1964.

51. Beattie, W. H., and Booth, C., J. Polymer Sci. 44:81-91(1960).

52. Beattie, W. H., and Booth, C., J. Phys. Chem. 64:696-7(1960).

53. Cabannes, J., and Rocard, Y. La diffusion moleculaire de la lumiere. Paris, Les Presses Universitaires de Paris, 1929.

54. Zimm, B. H., Stein, R. S., and Doty, P. M., Polymer Bull. 1:90(1945).

55. Timell, T. E. Wood hemicelluloses. Syracuse, New York, Syracuse University, 1963. 209 p.

56. Thompson, N. A. Personal communication.

57. Klages, F., and Niemann, R., Ann. 523:224-34(1936); C.A. 30:6711.

58. Gans, von R., and Tollens, B., Ber. dtsch. chem. Ges. 21:2150(1888).

59. Higler, A., Ber. 36:3197-203(1903).

60. Guzman, G. M., and Gomey-Fatau, J. M., Anales Real. Soc. Espan. Fis. Quim. (Madrid) 53B:669(1957).

61. Meyerhoff, G., J. Polymer Sci. 29:399-410(1958).

62. Ott, E., and Spurlin, H. M. Cellulose and cellulose derivatives. 2nd ed. New York, Interscience, 1955. 1607 p.

63. Palmer, K. J., and Ballantyne, M., J. Am. Chem. Soc. 72:736-41(1950).

64. Hunt, M. L., Newman, S., Scheraga, H. A., and Flory, P. J., J. Phys. Chem. 60:1278-90(1956).

65. Henley, D., Arkiv Kemi 18:327-92(1961).

66. Swenson, H. A., and Thompson, N. A. Personal communication.

67. Orofino, T. A., and Flory, P. J., J. Chem. Phys. 26:1067-76(1957).

68. Stockmayer, W. H., Makromol. Chem. 35:54-74(1960).

69. Krigbaum, W. R., and Sperling, L. H., J. Phys. Chem. 64:99-108(1960).

70. Notley, N. T., and Debye, P. J., J. Polymer Sci. 17:99-106(1955).

71. Benoit, H., J. Polymer Sci. 3:376-88(1948).

72. Burchard, W., and Husemann, E., Makromol. Chem. 44-46:358-87(1961).

73. Debye, P. Collected Papers. New York, Interscience, 1954.

74. Brown, W., Arkiv Kemi 18:227-84(1961).

75. Burchard, W., Makromol. Chem. 42:151-64(1960).

76. Trevelyan, W. E., Proctor, D. P., and Harrison, J. S., Nature 166:444-5 (1950).

77. Hough, L., Jones, J. K. N., and Wadman, W. H., J. Chem. Soc. 1950:1702-6.

78. Partridge, S. M., Nature 164:443(1949).

79. Burrell, H., Interchem. Rev. 14, no. 2:31-46(1955).

80. Linnell, W. Physicochemical properties of the triacetate derivative of the glucomannan from black spruce (Picea mariana). Progress Report 2. Appleton, Wis., The Institute of Paper Chemistry, 1964. 44 p.

APPENDIX I

DEVELOPERS, DIPS, AND SPRAYS USED IN PAPER CHROMATOGRAPHY

DEVELOPER

Solvent A, for resolution of neutral substances and for holding acidic materials near the starting line, was made by volume of 8 parts ethyl acetate, 2 parts pyridine, and 1 part water.

DIPS AND SPRAYS

SILVER NITRATE (76)

Three grams of silver nitrate was dissolved in 5-6 ml. of water, 95 ml. of acetone was added, and water was added dropwise to dissolve any precipitate. The chromatograms were dipped into this solution for 10 sec., air dried, and dipped into 0.5N sodium hydroxide in ethanol. They were permitted to stand at approximately 25°C. for 10 min. to allow the spots to develop, washed with 10% sodium thiosulfate to remove excess silver nitrate, washed with water, and air dried.

This reagent was used for all qualitative chromatography of the hydrolyzate obtained from total acid hydrolysis of the glucomannan.

p-ANISIDINE HYDROCHLORIDE (77)

The chromatograms were sprayed with the reagent, which was mixed in the following order: 0.5 g. of p-anisidine hydrochloride, 5 ml. of water, 10 ml. of ethanol, and 85 ml. of n-butanol. The chromatograms were air dried, and heated to 105°C. for 5 min. Pentoses were pink to red, and hexoses were brown.

This reagent was used for the qualitative chromatography of the hydrolyzates obtained from total and graded hydrolysis. It was also used in conjunction with the determination of the sugar ratios in the whole polymer and the barium-precipitated fractions.

ANILINE PHTHALATE (78)

Phthalic anhydride (8.3 g.) was dissolved in 500 ml. of water-saturated butanol, and just before spraying 1 ml. of aniline was added to 100 ml. of the solution. The sprayed chromatograms were air dried and heated at 105°C. for 3-5 min. Hexoses were yellow-brown and pentoses were red-brown. This reagent was used in conjunction with the quantitative determinations of the sugars in the glucomannan.

APPENDIX II

METHOD OF SOLVENT SELECTION

The systematic technique of using solubility parameters to select polymer solvents has proved to be of little or no value when selecting solvents for polysaccharides and their derivatives (8, 79). In selecting a solvent for a spruce glucomannan acetate, Linnell (80) found that the materials which were solvents or near solvents were capable of donating a proton, in the form of a plus dipole, to the proton-accepting carbonyl of the ester group of the polymer, and that all nonsolvents had little or no proton-donating character. These observations were not available until after the solvent for salep glucomannan triacetate had been selected, but they may be helpful in future selections of solvents for polysaccharide derivatives.

The solvent for salep glucomannan triacetate was selected after trying many potential solvents and selecting the one with the most desirable properties. In all cases the solvent was added to a small amount of polymer in a test tube. The mixture was shaken and placed aside for several days, with occasional shaking. If solubility was incomplete, the mixture was heated to 50-60°C. on a steam bath and set aside for another day. The final judgment was first made by visually examining the test tube to see whether the polymer had dissolved completely, partially, or not dissolved at all. Table XV gives a list of the potential solvents that were tried.

The twelve solvents that proved satisfactory for the glucomannan triacetate were examined with respect to toxicity, hygroscopicity, refractive index, density, and cost. Nitroethane and diethyl oxalate appeared to be the most desirable. Viscosity and light-scattering measurements in both solvents lead

to the final selection of nitroethane. Nitroethane yields a solution with a larger refractive index gradient than does diethyl oxalate and has a lower viscosity.

TABLE XV

POTENTIAL SOLVENTS TESTED IN THE SELECTION OF A SOLVENT FOR SALEP GLUCOMANNAN TRIACETATE

Satisfactory Solvents

2-Aminoethanol	Tetrafluoropropanol
2-Chloroethanol[a]	Dimethylsulfoxide
1,3-Chloro-2-propanol	Benzylamine
Trimethylene chlorohydrin	Nitroethane
1,1,2-Trichloroethane	Diethyl oxalate
1,2,3-Trichloropropane	Diethyl malonate

Unsatisfactory Solvents

P = Partially soluble with some swelling, but insoluble particles remaining.
I = Insoluble.

Esters	Solubility Index
Methyl acetate	P
Ethyl acetate	P
Propyl acetate	I
Butyl acetate	I
Methyl salicylate	I
Ethyl lactate	I
Triethyl citrate	P
Butyl phthalate	I
Butyl oxalate	P
Butyl tartrate	P
Diethyl carbonate	I
Ethers and Ketones	
Acetone	P
Dioxane	I
2-Methoxy ethanol	I
Tetrahydrofuran	P
2,4-Pentanedione	P
2,5-Hexanedione	P
2-Butanone	P

[a]Very toxic.

TABLE XV (Continued)

POTENTIAL SOLVENTS TESTED IN THE SELECTION OF A SOLVENT FOR SALEP GLUCOMANNAN TRIACETATE

Unsatisfactory Solvents (cont'd.)

Aromatics	Solubility Index
Nitrobenzene	P
Chlorobenzene	I
1,3-Dibromobenzene	I
Benzene	I
Toluene	I
Nitriles and Amines	
Acetonitrile	P
Chloroacetonitrile	P
Phenylacetonitrile	P
Benzoacetonitrile	P
Acrylonitrile	P
Pyridine	P
Formamide	P
n-Butylamine	P
Miscellaneous	
Methylene chloride[a]	P
Chloroform	P
Carbon tetrachloride	P
Trimethylene bromide	I
Trifluoroethanol	P
Carbon disulfide	I
Nitromethane	P

[a]Very toxic.

APPENDIX III

CALIBRATION OF VARIABLE SHEAR VISCOMETER AND SOLVENT EFFLUX TIMES

CALIBRATION OF THE VISCOMETER

In a capillary viscometer the viscosity may be calculated using the following form of the Poiseuille equation (37):

$$\eta = A\rho t - B\rho/t \qquad (30),$$

where η is the viscosity of a liquid of density ρ flowing through a capillary in time, t. A and B are constants for a given viscometer operating under a fixed mean hydrostatic head. Both constants incorporate the end effect correction (39), which is due to the convergence and divergence of flow lines at the capillary ends. The term $B\rho/t$ is the kinetic energy correction which accounts for the fact that part of the pressure difference between the capillary ends imparts kinetic energy to the emerging liquid. Most capillary viscometers are designed so that the kinetic energy correction is a minimum and can be neglected.

In order to determine the magnitude of the kinetic energy correction the values of A and B may be determined by writing Equation (30) in the form

$$\eta/\rho t = A - B/t^2 \qquad (31).$$

The values of A and B, respectively, may be obtained from the intercept and slope of a plot of $\eta/\rho t$ versus $1/t^2$. This was done for each bulb of the Cannon 47-A1 variable-shear viscometer using ethanol, water, methanol, and toluene as the calibration liquids. The results are shown in graphical form in Fig. 28 and given in tabular form in Table XVI.

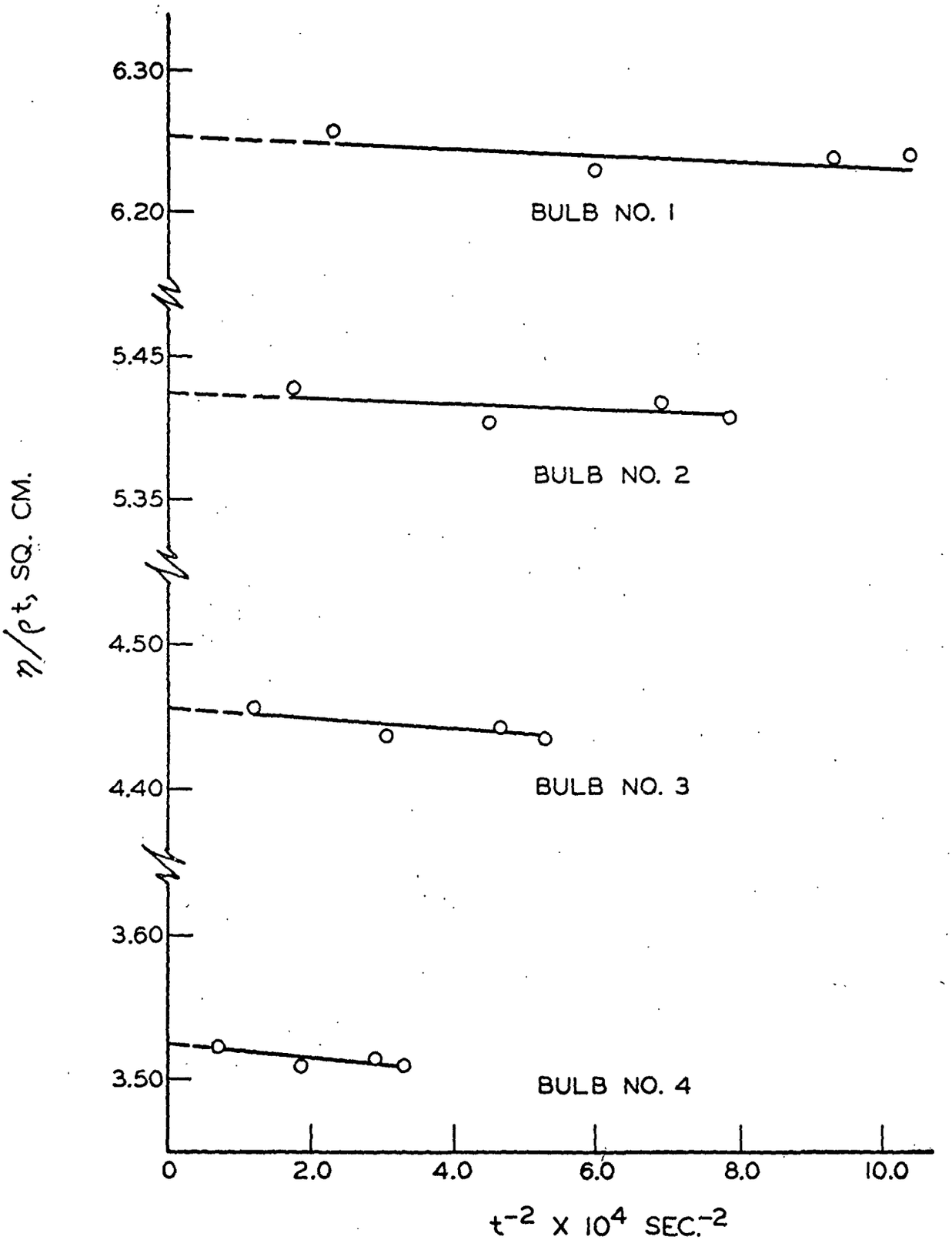

Figure 28. Calibration Curves for Cannon 47-Al Shear Viscometer

TABLE XVI

RESULTS OF CALIBRATION OF THE CANNON 47-A1 VISCOMETER

Bulb Number	$\underline{A} \times 10^5$ sq. cm./sec.^{2}	$\underline{B} \times 10^3$ sq. cm.	$\underline{X} \times 10^3$
1	6.25	2.12	3.60
2	5.43	2.20	3.26
3	4.46	3.76	4.54
4	3.52	4.57	4.37

KINETIC ENERGY CORRECTIONS WITH NITROETHANE

The fractional kinetic energy correction for the solvent is

$$X = (B\rho/t)\,(A\rho t) \qquad (32)$$

Column four of Table XVI gives the fractional kinetic energy correction for each bulb of the viscometer when the flow times for nitroethane are inserted into Equation (32). All corrections are less than 0.5% and are considered negligible. The efflux times for a number of solvents are given in Table XVII.

TABLE XVII

SOLVENT EFFLUX TIMES AT 30°C.

Solvent	Bulb 1, sec.	Bulb 2, sec.	Bulb 3, sec.	Bulb 4, sec.
Water	129.1	148.8	181.2	229.2
Nitroethane	94.9	109.2	133.4	168.3
Diethyl oxalate	247.1	284.7	347.1	439.7